Author's personal copy

Remote Sensing of Environment 114 (2010) 1968–1986

Contents lists available at ScienceDirect

Remote Sensing of Environment

journal homepage: www.elsevier.com/locate/rse

Grape quality assessment in vineyards affected by iron deficiency chlorosis using narrow-band physiological remote sensing indices

F. Meggio [a], P.J. Zarco-Tejada [b,*], L.C. Núñez [c], G. Sepulcre-Cantó [b], M.R. González [c], P. Martín [c]

[a] Department of Environmental Agronomy and Crop Science, University of Padova, Italy
[b] Instituto de Agricultura Sostenible (IAS), Consejo Superior de Investigaciones Científicas (CSIC), Córdoba, Spain
[c] Departamento de Producción Vegetal y Recursos Forestales, ETS de Ingenierías Agrarias, Universidad de Valladolid, Palencia, Spain

ARTICLE INFO

Article history:
Received 1 December 2009
Received in revised form 7 April 2010
Accepted 10 April 2010

Keywords:
Hyperspectral remote sensing
Radiative transfer
Physiological indices
Stress detection
Airborne remote sensing

ABSTRACT

The present study investigated the use of physiological indices calculated from hyperspectral remote sensing imagery as potential indicators of wine grape quality assessment in vineyards affected by iron deficiency chlorosis. Different cv. Tempranillo/110 Richter vineyards located in northern Spain, affected and non-affected by iron chlorosis, were identified for field and airborne data collection. Airborne campaigns imaged a total of 14 study areas in both 2004 and 2005 using the AHS hyperspectral sensor, which acquired 20 spectral bands in the VIS-NIR region. Field measurements were conducted in each study site to obtain leaf and grape physiological parameters potentially linked to wine quality. Simulations carried out with the rowMCRM radiative transfer model demonstrated the feasibility of estimating leaf chlorophyll a + b (C_{ab}) content using TCARI/OSAVI from AHS spectral bands. In addition to traditional structural vegetation indices (NDVI) and successful canopy-level chlorophyll indices (TCARI/OSAVI), other innovative physiological indices sensitive to changes in carotenoid (*Car*) and anthocyanin (*Anth*) content in leaves were assessed from the imagery. The rowMCRM model simulations were used to evaluate canopy structural effects on these physiological indices as a function of the typical row-structured canopy variables in vineyards (LAI, crown width, row distances, C_{ab} content and soil background effects). Modeling results concluded that *Car* (Gitelson-*Car2*) and *Anth* (Gitelson-*Anth*) indices were highly affected by canopy structure (C_w, V_s) and soil background (ρ_s). Field measurements of grape composition and quality were used to assess potential relationships with physiological indices sensitive to foliar pigment content (C_{ab}, *Car* and *Anth*). NDVI and TCARI/OSAVI indices yielded lower relationships for CIRG and IMAD must quality parameters than *Car* and *Anth* physiological indices. These results suggest that the increase in carotenes and anthocyanins due to drought, thermal damage or micronutrient deficiencies is a better indicator to detect phenolic ripening difficulties for vines affected by iron chlorosis than chlorosis detection. Therefore, the potential use of physiological remote sensing indices related to carotene and anthocyanin pigments demonstrates their importance as grape quality indicators in vineyards affected by iron chlorosis.

© 2010 Elsevier Inc. All rights reserved.

1. Introduction

Iron deficiency is an important constraint in grape growing in Mediterranean climate areas. Iron deficiency decreases chlorophyll and carotenoid concentration per area in leaves (chlorosis), damaging the structure and function of the photosynthetic apparatus (Terry & Abadia, 1986). The low photosynthesis rate occurring in chlorotic plants considerably depresses the yield and vigor of vineyards (Chen & Barak, 1982; Tagliavini & Rombolà, 2001). Iron chlorosis also leads to poor wine grape quality, reducing sugar and anthocyanin contents (Castino et al., 1987; Veliksar et al., 2005).

Grape composition plays a critical role in wine quality. In must, a large portion of the soluble solids is sugars, which determine the wine alcoholic degree. After sugars, organic acids are the most abundant solids present in grape juice. They are responsible for the tart taste and markedly influence a wine's stability and color. The aroma is created by various volatile compounds accumulated in the fruit during the ripening process and is highly dependent on environmental conditions. Phenolic compounds (anthocyanins and tannins) are present especially in skins and seeds, and determine the color and astringency of red wines. Anthocyanins are specific to red grapes and primarily responsible for wine color intensity and stability. Tannins contribute significantly to mouth-feel and color stability in red wines. Cultivar, fruit maturity, environmental conditions such as climate and soil, vineyard management practices, and the interactions among these

* Corresponding author. Instituto de Agricultura Sostenible (IAS) Consejo Superior de Investigaciones Científicas (CSIC) Alameda del Obispo, s/n 14004-Córdoba Spain. Tel.: +34 957 499 280, +34 676 954 937; fax: +34 957 499 252.
E-mail address: pzarco@ias.csic.es (P.J. Zarco-Tejada).
URL: http://www.ias.csic.es/pzarco (P.J. Zarco-Tejada).

0034-4257/$ – see front matter © 2010 Elsevier Inc. All rights reserved.
doi:10.1016/j.rse.2010.04.004

Author's personal copy

Fig. 1. Examples of images of three study sites acquired in the 2004–2005 campaigns with the Airborne Hyperspectral Scanner (AHS). The images were collected at 2.5 m spatial resolution.

factors result in the composition and final potential quality of grapes (Johnson et al., 2001; Lamb et al., 2004).

The synthesis and accumulation of sugars, acids and phenolic compounds in grapes through ripening is greatly influenced by the photosynthetic capacity of the vines (Pirie & Mullins, 1980; Smart & Robinson, 1991). This capacity depends directly on vine-leaf biomass (canopy size, density and vigor) and leaf chlorophyll content (Hall et al., 2002). Research efforts in precision viticulture demonstrate the feasibility of remote sensing as a consistent method to estimate these parameters in vineyards, as potential indicators of yield (Lamb et al., 2001) and fruit and wine composition (Johnson et al., 2001; Lamb et al., 2004; Martín et al., 2007). Precision viticulture techniques aim at pointing out homogeneous zones based on remotely sensed biophysical variable estimates, enabling inter- and within-field variability detection in vineyards and the generation of maps with a gradient of management zones potentially linked to wine quality. Previous studies showed that vineyard vigor could be successfully mapped using high spatial IKONOS satellite imagery (Johnson et al., 2003), enabling vine growth monitoring for irrigation support and canopy management through temporal relationships between the

Table 1
Hyperspectral vegetation and physiological indices used in this study.

Index	Index-ID	Equation	References
Leaf area index			
Normalized difference vegetation index	NDVI	$NDVI = (R_{NIR} - R_{red})/(R_{NIR} + R_{red})$	Rouse et al. (1974)
Chlorophyll estimation			
Transformed C_{ab} absorption in reflectance index	TCARI	$TCARI = 3*[(R_{700} - R_{670}) - 0.2*(R_{700} - R_{550})*(R_{700}/R_{670})]$	Haboudane et al. (2002)
Optimized soil-adjusted vegetation index	OSAVI	$OSAVI = (1 + 0.16)*(R_{800} - R_{670})/(R_{800} + R_{670} + 0.16)$	Rondeaux et al. (1996)
	TCARI/OSAVI	TCARI/OSAVI	Haboudane et al. (2002)
	Gitelson-*Chl*1	$[R_{(540-560)}^{-1} - R_{(760-800)}^{-1}]*R_{(760-800)}$	Gitelson et al. (2003, 2006)
	Gitelson-*Chl*2	$[R_{(690-720)}^{-1} - R_{(760-800)}^{-1}]*R_{(760-800)}$	Gitelson et al. (2003, 2006)
Carotenoid estimation			
Simple ratio	Chappelle-*Car*	R_{760}/R_{500}	Chappelle et al. (1992)
Simple ratio	Blackburn-*Car*1	R_{800}/R_{470}	Blackburn (1998)
	Blackburn-*Car*2	$(R_{800} - R_{470})/(R_{800} + R_{470})$	Blackburn (1998)
Structure-Intensive Pigment Index (SIPI)	SIPI	$SIPI = (R_{800} - R_{445})/(R_{800} + R_{680})$	Peñuelas et al. (1995)
	Gitelson-*Car*1	$[R_{(510-520)}^{-1} - R_{(540-560)}^{-1}]*R_{(760-800)}$	Gitelson et al. (2003, 2006)
	Gitelson-*Car*2	$[R_{(510-520)}^{-1} - R_{(690-710)}^{-1}]*R_{(760-800)}$	Gitelson et al. (2003, 2006)
Anthocyanin estimation			
	Gamon-*Anth*	$R_{600-700}/R_{500-600}$	Gamon and Surfus (1999)
	Gitelson-*Anth*	$[R_{(540-560)}^{-1} - R_{(690-710)}^{-1}]*R_{(760-800)}$	Gitelson et al. (2003, 2006)

Author's personal copy

Table 2
Hyperspectral vegetation and physiological indices calculated using AHS imagery.

Index-ID	AHS imagery adapted indices
Leaf area index	
NDVI	$NDVI = (R_{804} - R_{659})/(R_{804} + R_{659})$
Chlorophyll	
TCARI	$TCARI = 3*[(R_{718} - R_{689}) - 0.2*(R_{718} - R_{571})*(R_{718}/R_{689})]$
OSAVI	$OSAVI = (1 + 0.16)*(R_{804} - R_{689})/(R_{804} + R_{689} + 0.16)$
TCARI/OSAVI	TCARI/OSAVI
Gitelson-*Chl*1	$[R_{571}^{-1} - R_{746}^{-1}]*R_{746}$
Gitelson-*Chl*2	$[R_{689}^{-1} - R_{746}^{-1}]*R_{746}$
Carotenoid	
Chappelle-*Car*	R_{746}/R_{513}
Blackburn-*Car*1	R_{804}/R_{484}
Blackburn-*Car*2	$(R_{804} - R_{484})/(R_{804} + R_{484})$
SIPI	$SIPI = (R_{804} - R_{455})/(R_{804} + R_{689})$
Gitelson-*Car*1	$[R_{484}^{-1} - R_{571}^{-1}]*R_{746}$
Gitelson-*Car*2	$[R_{484}^{-1} - R_{689}^{-1}]*R_{746}$
Anthocyanin	
Gamon-*Anth*	R_{659}/R_{571}
Gitelson-*Anth*	$[R_{571}^{-1} - R_{689}^{-1}]*R_{804}$

Normalized Difference Vegetation Index (NDVI) and the Leaf Area Index (LAI). This vegetation index and other ratios derived from field data and multispectral aerial photography were tested in recent studies to estimate canopy cover and dormant pruning weight, obtaining consistency across growing seasons (Dobrowski et al., 2002, 2003; Hall et al., 2008). These and other studies suggested broad-band multispectral remotely sensed imagery of high spatial resolution as a potential method for vineyard canopy structure characterization, enabling a successful estimation of vine canopy size, shape and row identification (Hall et al., 2003), vine mortality detection (Lagacherie et al., 2001), vineyard classification methods (Lanjeri et al., 2001) and vine canopy cover estimation for irrigation management support (Montero et al., 1999). In this context, further research efforts were performed exploring high spatial resolution hyperspectral remote sensing imagery and physical methods to estimate biochemical constituents and biophysical variables as a means to assess within-field vine status and function (Zarco-Tejada et al., 2003, 2005; Martín et al., 2007).

A deeper understanding of leaf and canopy reflectance has favored the development of remote sensing applications for agriculture (Hatfield et al., 2008). Leaf biochemistry, such as the concentration

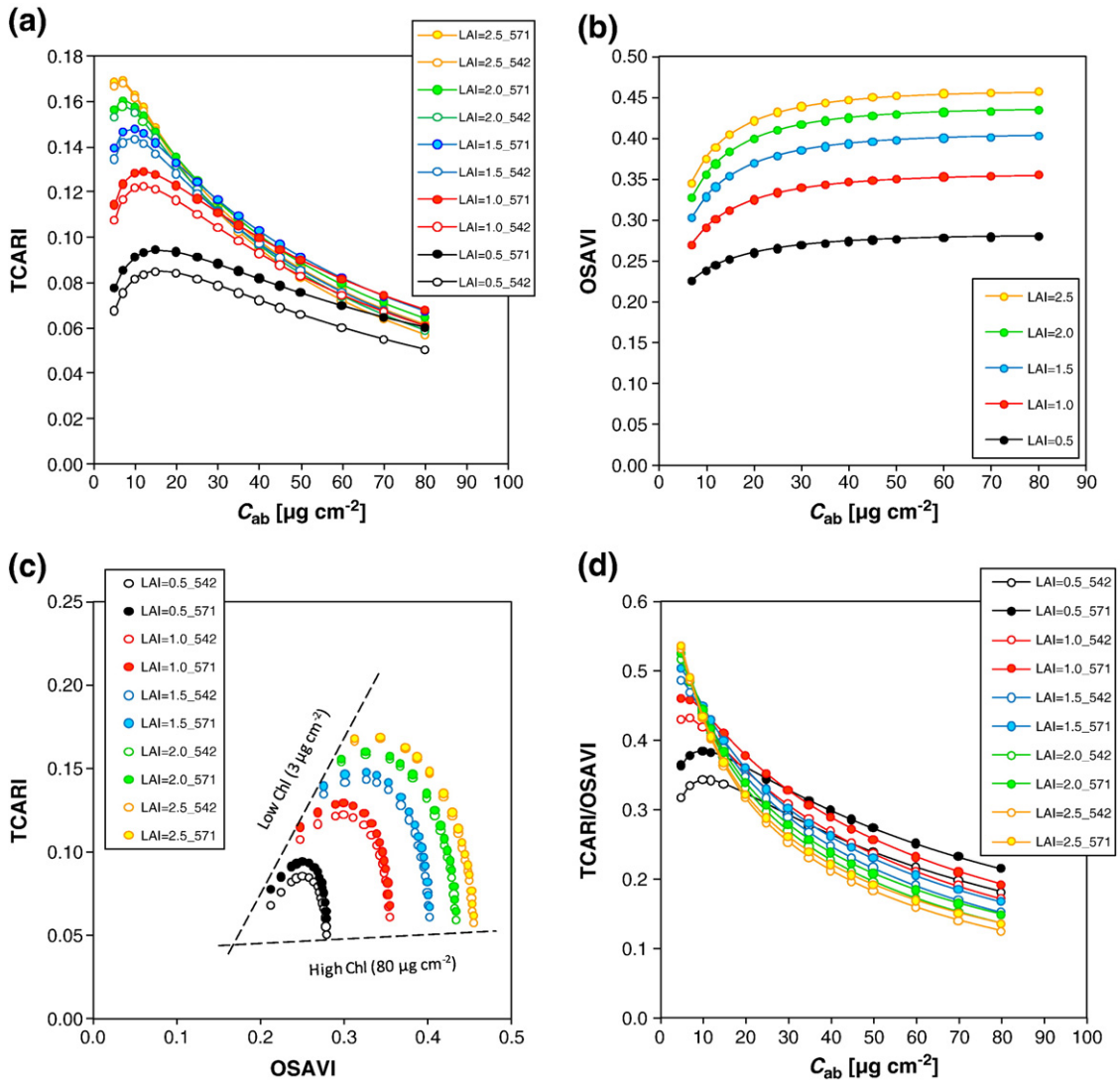

Fig. 2. Modeling simulations performed with rowMCRM to achieve effects of LAI on TCARI, OSAVI and TCARI/OSAVI sensitivity to chlorophyll variations using bands 571 nm instead of 542 nm in the TCARI index calculation.

Author's personal copy

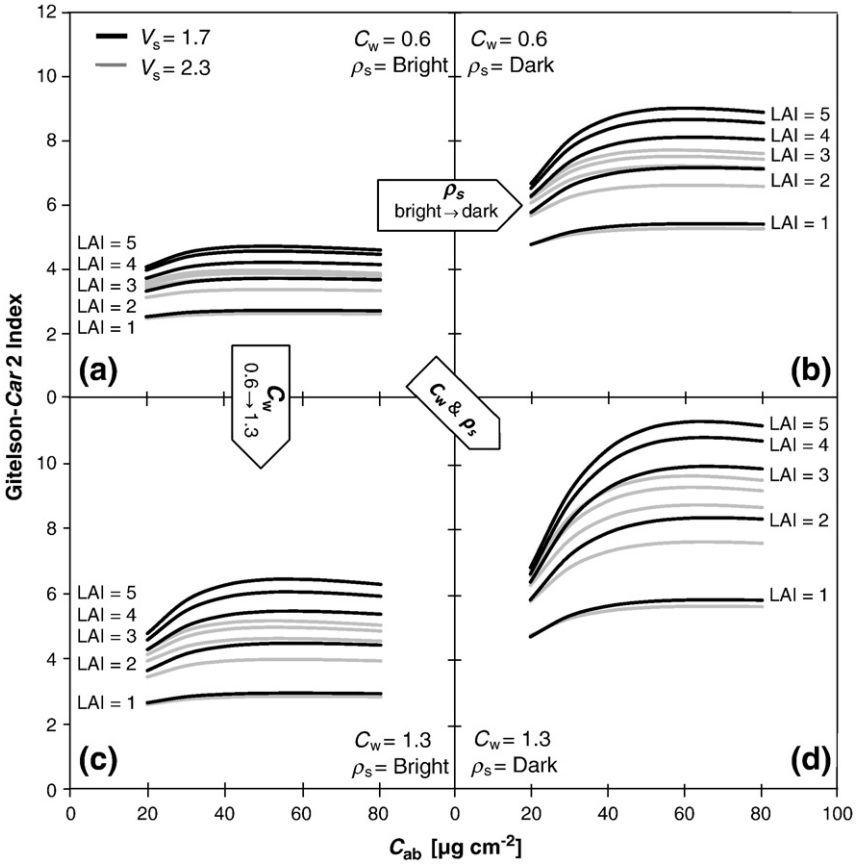

Fig. 3. Modeling simulations performed with rowMCRM to achieve the effect of soil background, LAI, vine width and visible soil strip on Gitelson-*Car*2 index sensitivity to chlorophyll content variation (C_{ab}).

of chlorophyll a + b (C_{ab}), water (C_w) and dry matter (C_m), is a physiological indicator of plant growth and stress status which can be estimated by empirical methods (indices) and analytical techniques (physical methods) from remote sensing data in the 400–2500 nm spectral region. Recent studies indicate that the estimation of leaf biochemical characteristics may be used as an indicator of vegetation chlorosis due to plant stress from nutritional deficiencies (Fernández-Escobar et al., 1999; Jolley & Brown, 1994; Marschner et al., 1986; Tagliavini & Rombolà, 2001; Wallace, 1991). One of the most important biochemical constituents for understanding plant physiological status is $C_{ab,}$ which is involved in solar light energy absorption and provides the mechanism for photosynthetic reactions. Thus, C_{ab} is directly linked to photosynthetic potential and primary production, and its content in leaves is closely related to plant stress and senescence processes. Leaf C_{ab} concentration can be detected by photosynthetic pigment responses in leaf reflectance in the green peak and along the red-edge spectral region (Rock et al., 1988; Vogelmann et al., 1993; Carter, 1994; Gitelson et al., 1996).

In particular, C_{ab} estimation for chlorosis detection in vegetation has been assessed in several studies based on spectroscopy and leaf optical properties using reflectance indices, spectral and derivative indices, derivative ratios in the red-edge region (Carter & Spiering, 2002; Gitelson et al., 2003; Jacquemoud et al., 1996; le Maire et al., 2004; Sims & Gamon, 2002; Richardson et al., 2002) and new optical indices derived from high resolution hyperspectral imagery (Carter, 1994; Gitelson & Merzlyak, 1996; Vogelmann et al., 1993; Zarco-Tejada et al., 2001, 2004, 2005). In later studies, the combination of indices based on the Transformed Chlorophyll Absorption in Reflectance Index (TCARI) (Haboudane et al., 2002), the Modified Chlorophyll Absorption in Reflectance Index (MCARI) (Daughtry et al., 2000), and the Optimized Soil-Adjusted Vegetation Index (OSAVI) (Rondeaux et al., 1996), such as TCARI/OSAVI and MCARI/OSAVI, has been demonstrated robust to soil background and leaf area index (LAI) variation in crops. These narrow-band indices, linked to radiative transfer simulations, provided useful predictive relationships for precision agriculture applications with hyperspectral imagery in continuous crop canopies (Haboudane et al., 2002) and have been adapted to open-tree canopy orchards (Zarco-Tejada et al., 2004; Meggio et al., 2008). Estimation of leaf biochemical constituents in row-structured crop canopies requires, in fact, appropriate modeling methods to account for row orientation and sun geometry, which affect the proportions of shadows, sunlit and shaded soil, and pure vegetation scene components (Zarco-Tejada et al., 2005). Differences in row-crop structural parameters, such as row height, row width, row LAI, varying soil backgrounds, and visible soil proportion, were assessed using hyperspectral imagery (Zarco-Tejada et al., 2005) to demonstrate their important effects on canopy reflectance and therefore estimation of C_{ab}. In addition, different sun viewing geometries (i.e., sun azimuth and zenith angles) have a greater influence on the optical vegetation index and the estimated leaf biochemical constituents in row-structured canopies (Meggio et al., 2008).

While most predictive relationships between leaf reflectance and pigment content have been developed for C_{ab} content estimation, providing quite robust predictions, only few models support carotenoid (*Car*) and anthocyanin (*Anth*) content estimation (Chappelle et al., 1992; Peñuelas et al., 1995; Blackburn, 1998; Gamon & Surfus, 1999; Fuentes et al., 2001; Sims & Gamon, 2002; Gitelson et al., 2001,

Author's personal copy

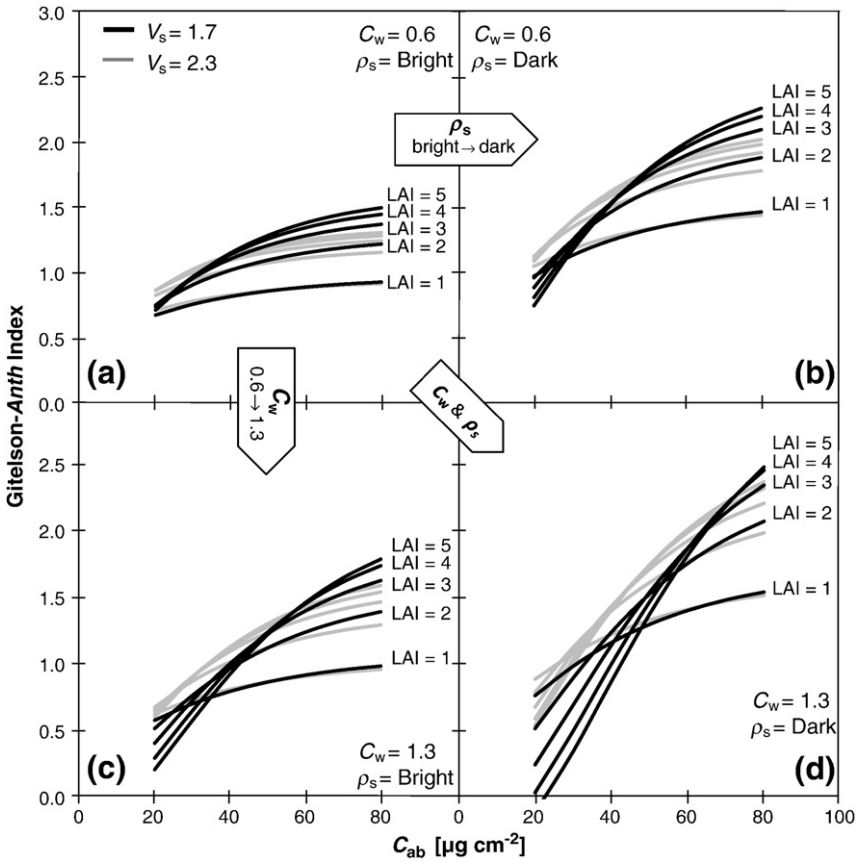

Fig. 4. Modeling simulations performed with rowMCRM to achieve the effect of soil background, LAI, vine width and visible soil strip on Gitelson-*Anth* index sensitivity to chlorophyll content variation (C_{ab}).

2002, 2006). *Car* and C_{ab} are the main pigments of green leaves for light harvesting, also playing a photo-protective role to prevent damage to the photosynthetic systems (Dawson et al., 1998; Gitelson et al., 2002; Merzlyak et al., 2003). *Anth*, the red pigments, protect leaves from excess light (Merzlyak & Chivkunova, 2000; Gitelson et al., 2002, 2006) and are often observed under environmental stresses such as high temperature, drought and mineral deficiencies (Chalker-Scott, 1999; Harbone, 1976). Recent studies developed physiological indices obtaining consistent relationships with *Car* (Peñuelas et al., 1995; Fuentes et al., 2001; Sims & Gamon, 2002; Gitelson et al., 2003, 2006) and *Anth* leaf pigments (Gamon & Surfus, 1999; Gitelson et al., 2006). As *Car* and *Anth* pigment concentrations are linked to photosynthetic efficiency, which affects fruit composition, physiological indices sensitive to pigment content could be used to detect spatial differences in fruit quality. In calcareous soils, iron availability can be one of the major factors modifying canopy size and foliar pigment content in leaves, which have considerable spatial variation in vineyards affected by chlorosis (Zarco-Tejada et al., 2005). Work conducted by Zarco-Tejada et al. (2005) and Martín et al. (2007) demonstrated that estimation of C_{ab} concentration at canopy level using remote sensing methods can be useful to map grape quality in vineyards affected by iron chlorosis. However, physiological indices linked to *Car* and *Anth* may yield in these areas superior results compared to other indices linked to vegetative vigor (NDVI) and C_{ab} content (TCARI/OSAVI). Therefore, research is needed on physiological condition detection using narrow-band hyperspectral remote sensing imagery. In fact, such physiological indices linked to *Car* and *Anth* have not yet been tested in vineyards for stress detection and grape quality assessment.

The objective of this investigation was to evaluate the use of physiological indices calculated from hyperspectral remote sensing imagery as potential indicators of wine grape quality assessment in vineyards affected by iron deficiency chlorosis.

2. Material and methods

2.1. Study site description

Data acquisition campaigns were conducted in July 2004 and 2005 in the western area of Ribera del Duero *Appellation d'Origine* (northern Spain). A total of seven full production vineyards, affected and non-affected by iron deficiency chlorosis, were selected for ground measurements during both years. Field data collection involved a total of 5 sub-areas of 10 m × 10 m located in each of the 7 vineyards. The study sites used for ground and airborne data collection were based on a plot network currently monitored by the local government, with specific sites selected to assure that an appropriate variability in leaf biochemistry and vine physiological conditions was found across the sites. The soils are calcareous, poor in organic matter (about 7.6 g·kg^{-1}), with a medium-weighed texture and an average pH of 8.7. Concentrations of active carbonate (up to 17.6%) and DPTA extractable Fe (1.2 to 7.6 mg·kg^{-1}) are highly heterogeneous within the area. Rainfall recorded in the study area was 358 mm in 2004 and 306 mm in 2005. All vineyards corresponded to cv. Tempranillo grafted on 110-Richter rootstock, with ages ranging between 7 and 16 years. Vine density ranged between 2200 and 4000 vines per hectare, and plants were trained to a simple or double Cordon Royat system (as described in detail in Martín et al., 2007). The vineyards

Author's personal copy

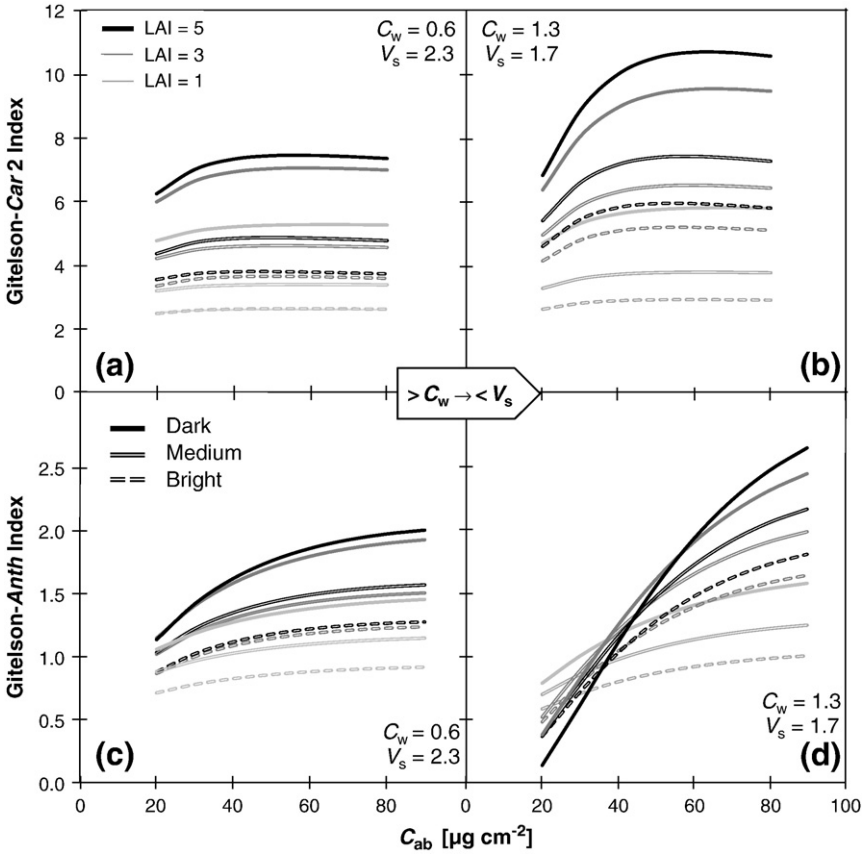

Fig. 5. Modeling simulations performed with rowMCRM to achieve the effect of soil background, LAI, vine width and visible soil strip on Gitelson-*Car*2 and Gitelson-*Anth* indices sensitivity to chlorophyll content variation (C_{ab}).

differed in canopy structure and soil background, and planting row orientation ranged from 0° to 180 °N, with the row direction angle measured clockwise from north.

2.2. Physiological measurements

Field sampling campaigns were conducted in these areas concurrent with airborne overflights, comprising canopy structural parameters (grid size, number of vines within each 10 m × 10 m plot, trunk height, plant height and width, and row orientation), soil chemical and structural analysis and leaf C_{ab} content determinations (Zarco-Tejada et al., 2005; Martín et al., 2007; Meggio et al., 2008). The leaf area index (LAI) and sunlit canopy cover in each study area were measured as described in Pérez (2002) and Carbonneau (1995), respectively. Forty leaf samples were collected at veraison in the study zones (OIV, 1996) to determine macro- and micronutrient contents in petioles. Yield and vigor (pruning weight) of the vines were also determined.

One week before harvest, when the mean value of total soluble solid content of must in all study plots reached 228 g·L^{-1}, a total of 100 berries from each study area were collected and the must used to determine the total soluble solids content (°Brix, total acidity (TA), tartaric and malic acid content, total polyphenols index (TPI), pH, color density and hue, in accordance with the European official methods of analysis (European Commission, 1990). In addition, a total of 100 berries collected in 2005 were sampled and their skins removed from pulp and seeds. The solid fraction was subjected to a process of extraction of polyphenolic compounds to determine the total polyphenols (Singleton & Rossi, 1965), anthocyanins (García-Barceló, 1990), tannins (Bate-Smith, 1954), and catechin content (Swain & Hillis, 1959), while also obtaining the polymerization degree of condensed tannins (DMACH index) (Vivas et al., 1994). The extraction of polyphenolic compounds was conducted with 7.5 ml of distilled water, adding to the skins of 100 berries a total of 10 ml of acid hydroalcoholic solution (10% ethanol, 5 g L^{-1} tartaric acid). The pH was adjusted with sodium hydroxide to a value of 3.6, and 32.5 ml of distilled water were added, keeping the mixture at 35 °C with slugging for 4 hours. The sample was cooled, centrifuged at 2000 g for 5 min and filtered through glass wool.

The color of musts and skin extracts was evaluated with a JASCO V-530 UV/VIS spectrophotometer. The coordinates $L^*a^*b^*$ were recorded using the D65 Illuminant as a reference (CIE, 1986). The Chromatic Index for Red Grapes (CIRG = $(180 - H^*)/(L^* + C^*)$), described by Carreño et al. (1995), was calculated.

2.3. Airborne campaigns and remote sensing physiological indices

Two years of imagery were acquired over experimental vineyards in collaboration with the Spanish Aerospace Institute (INTA) using the Airborne Hyperspectral Scanner (AHS), developed by Sensytech Inc. (currently Argon ST Inc., USA). Airborne campaigns were conducted in two consecutive years, 21 July 2004 and 21 July 2005, to acquire hyperspectral images over each vineyard. Images from both years were obtained at similar sun angles to minimize differences due to *bi-directional* reflectance (BRDF) effects between the years (2004, 07:45–8.22 GMT; 2005, 09:03–09:33 GMT). Fig. 1 shows a selection of 3 vineyard fields used in this study and imaged by the AHS airborne sensor. The hyperspectral imagery was acquired over the vineyard

Author's personal copy

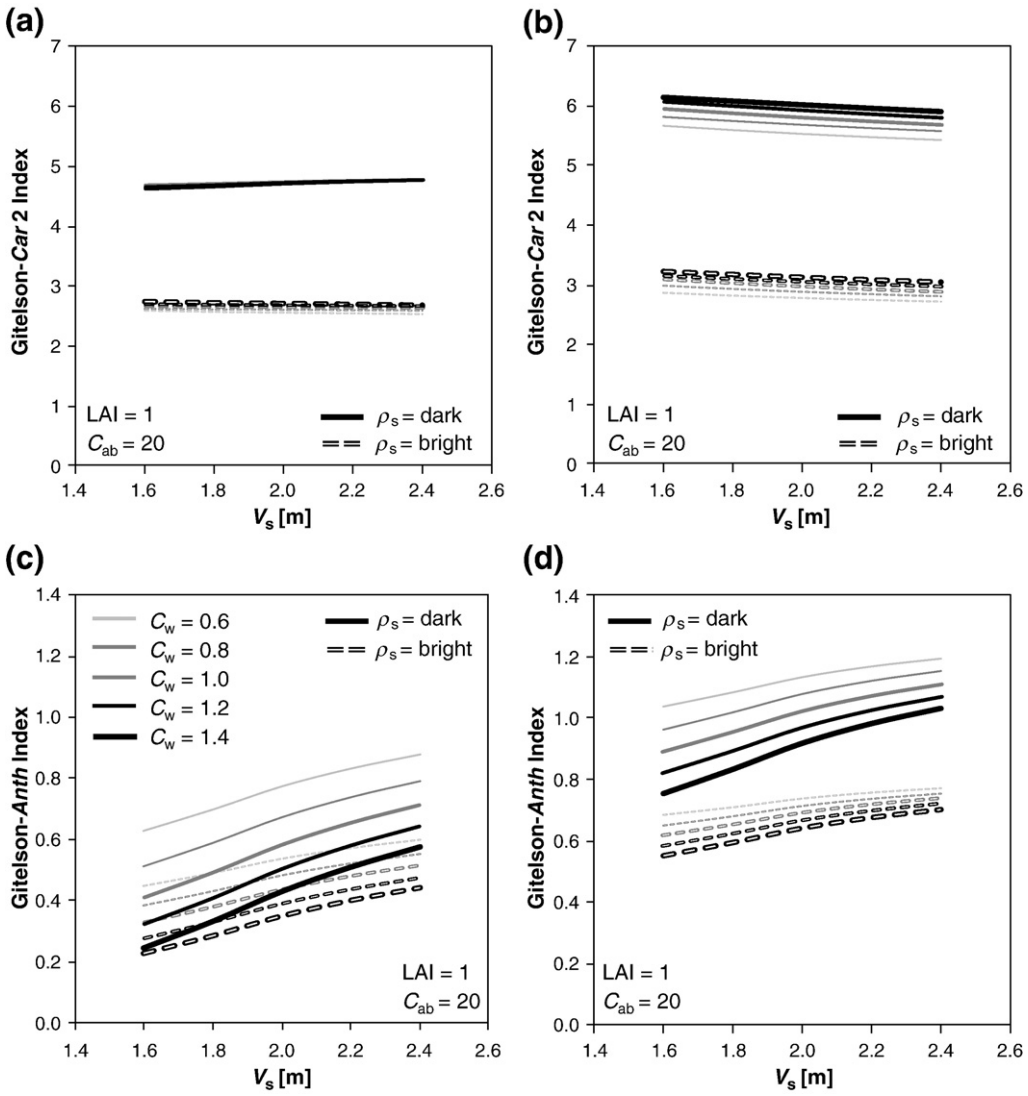

Fig. 6. Modeling simulations performed with rowMCRM to achieve the effect of the actual inter- and within-field variation of soil background (ρ_s), vine width (C_w) and chlorophyll content (C_{ab}) on Gitelson-*Car*2 and Gitelson-*Anth* indices sensitivity to visible soil strip variations (V_s).

fields at a flight altitude of 1000 m above ground level, obtaining images with a 90° field of view (FOV) and a 2.5 mrad instantaneous FOV (IFOV) lens, resulting in a spatial resolution of 2.5 m. The AHS sensor comprises 80 spectral bands in the 0.43–12.5 μm spectral range distributed in 4 ports (VIS/NIR, SWIR, MWIR and TIR). In this study, the VIS/NIR port was used, obtaining imagery with 20 bands over the 0.43–1.65 μm spectral range with a *full-width at half-maximum* (FWHM) of 30 nm.

The airborne flights were kept in the solar plane to minimize shadows, designing each overpass to image the study sites at nadir view. Images were processed by applying geometric, radiometric and atmospheric corrections. Imagery atmospheric correction was conducted using the *Simple Model of Atmospheric Radiative Transfer of Sunshine* (SMARTS) (Gueymard, 1995). Water vapor atmospheric content was obtained by scaling to the flight altitude the measured values at the 'Valladolid' and 'Palencia' sites as part of the AERONET network (http://aeronet.gsfe.nasa.gov). A full description of the calibration of the AHS bands and the radiometric and atmospheric corrections was provided in Sobrino et al. (2006). For the VIS/NIR region, soil reflectance spectra measured for each site at ground level were used to perform a *flat-field* correction (Ben-Dor & Levin, 2000) after atmospheric correction, which compensated for residual effects on derived surface reflectance images estimations in the atmospheric water and oxygen absorption spectral region.

Vegetation indices were calculated from each study site to assess changes in canopy structure and foliar pigment concentration as a function of vine status and grape quality parameters. The *Normalized Difference Vegetation Index* (NDVI) (Rouse et al., 1974) was calculated to track changes in canopy structure given its relationship with leaf area index. The *Transformed Chlorophyll Absorption in Reflectance Index* (TCARI) (Haboudane et al., 2002), based on the *Modified Chlorophyll Absorption in Reflectance Index* (MCARI) (Daughtry et al., 2000) and normalized by the *Optimized Soil-Adjusted Vegetation Index* (OSAVI) (Rondeaux et al., 1996) to obtain TCARI/OSAVI, was used in this study, as it has been demonstrated to successfully minimize soil background and leaf area index variations in crops, providing predictive relationships for chlorophyll concentration estimation with hyperspectral imagery in closed crops (Haboudane et al., 2002) and open tree canopy orchards (Zarco-Tejada et al., 2004; Meggio et al., 2008).

In addition to these *traditional* vegetation indices, other indices more closely related to physiology were calculated through the combination of reflectance bands in the visible spectral region

Author's personal copy

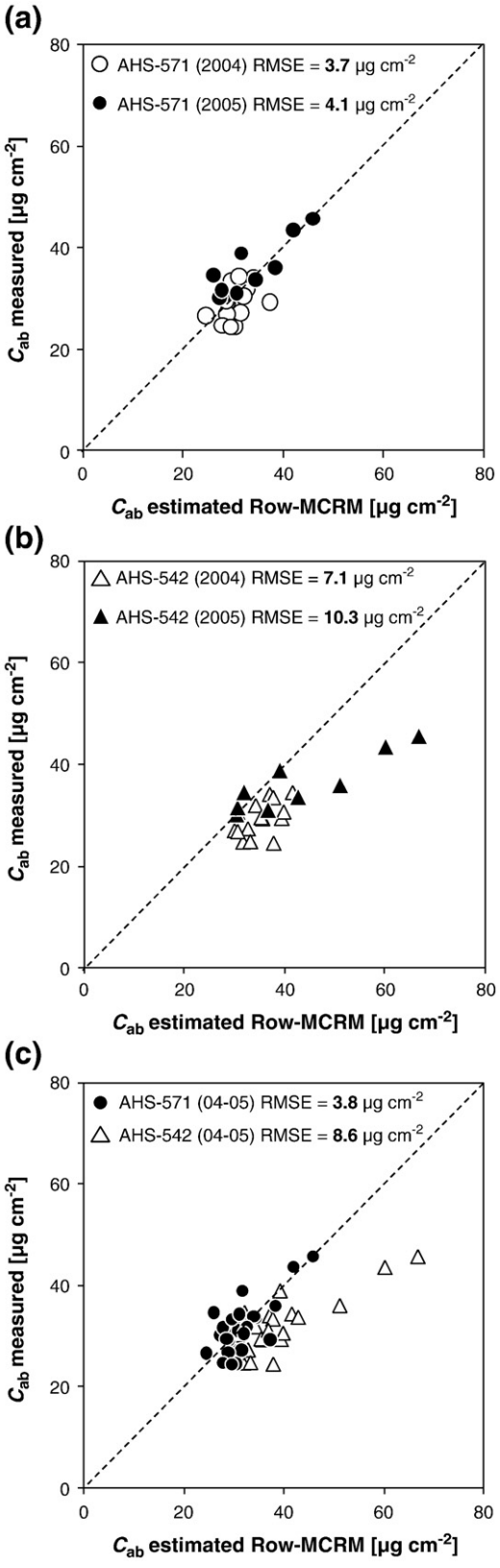

Fig. 7. Estimation of C_{ab} content at canopy level using TCARI/OSAVI through the rowMCRM model utilizing the predictive relationship proposed in Meggio et al. (2008). Differences between AHS band 571 and 542 nm for TCARI/OSAVI calculation for C_{ab} estimation.

(Gitelson et al., 2003, 2006; Chappelle et al., 1992; Blackburn, 1998; Peñuelas et al., 1995; Gamon & Surfus, 1999). These physiological indices have been proposed to track changes due to pigment content such as chlorophyll (C_{ab}), carotenoid (*Car*) and anthocyanin (*Anth*). In this study, different types of indices were used as a function of sensitivity to different parameters: leaf area index (NDVI), C_{ab} content (TCARI, OSAVI, TCARI/OSAVI, Gitelson-*Chl*1, Gitelson-*Chl*2), *Car* content (Chappelle-*Car*, Blackburn-*Car*1, Blackburn-*Car*2, SIPI, Gitelson-*Car*1, Gitelson-*Car*2) and *Anth* content (Gamon-*Anth*, Gitelson-*Anth*) (Table 1). The indices were adapted to enable calculation with AHS imagery (Table 2).

2.4. Modeling vineyard structural effects on physiological indices at the image level

Previous work demonstrates that C_{ab} content can be estimated using airborne CASI imagery through a modeling methodology to account for vineyard structure (Zarco-Tejada et al., 2003; Meggio et al., 2008). In this study, a different airborne sensor was flown over the vineyard fields, thereby requiring a simulation and validation study to assess the feasibility of the AHS bands for C_{ab} and other pigment estimation in vineyards. Previous studies, conducted with the AHS airborne sensor on PRI index changes associated with the *de-epoxidation* of the xanthophyll pigment cycle (Gamon et al., 1992), demonstrated the feasibility of the AHS bandset for TCARI/OSAVI, PRI and NDVI calculation (Zarco-Tejada et al., 2000; Suárez et al., 2008). In particular, the use of the 542 nm and 571 nm bands from the AHS airborne sensor for TCARI calculation was assessed, as the AHS bandset required a slight modification of the bands used for indices such as TCARI/OSAVI.

The MCRM model (Kuusk, 1995a,b), with additions to simulate the row vineyard structure (rowMCRM) (described in detail in Zarco-Tejada et al., 2005), was used to simulate TCARI and consequently TCARI/OSAVI sensitivity to C_{ab} with both AHS 571 nm and 542 nm bands (Fig. 2). Simulated spectra were calculated for 5 LAI values (0.5–2.5 in 0.5 steps), 15 leaf C_{ab} content levels (5–80 $\mu g \cdot cm^{-2}$ in 5 $\mu g \cdot cm^{-2}$ steps) using other rowMCRM inputs retrieved from specific data from Zarco-Tejada et al. (2003) and Meggio et al. (2008). TCARI and TCARI/OSAVI indices were calculated for each simulated spectrum using band 571 nm and 542 nm separately. The effects of plant growth (LAI) and leaf C_{ab} content on TCARI and OSAVI are illustrated in Fig. 2a, b.

As observed in Haboudane et al. (2002), LAI exerts a strong influence on the relationships between both TCARI and OSAVI and foliar pigment contents. The effects of different AHS bands used for TCARI calculation are remarkable, especially at low foliage cover (LAI<1) (Fig. 2c, d). In particular, Fig. 2c shows the chlorophyll index that TCARI plotted against OSAVI for various pigment content and LAI levels, as shown in Haboudane et al. (2002), to uncouple the effects of LAI and leaf pigments separately. Both indices appear, as expected, positively correlated with LAI (low TCARI and OSAVI values correspond to low LAI values and vice versa). The different band used (542 nm, 571 nm) for TCARI calculation shows critical effects only at low LAI values (LAI<1), which is important in the case of vineyard canopies. The TCARI/OSAVI index simulated with both AHS bands was then calculated, showing the trend for C_{ab} variability as a function of LAI (Fig. 2d). The simulation study enabled the selection of the AHS band 571 nm for TCARI calculation in the *scaling-up* relationship methodology proposed in Meggio et al. (2008) for C_{ab} content estimation.

The rowMCRM model was used for simulating *Car* and *Anth* physiological indices in order to assess canopy structural effects on the indices as a function of the typical row-structured canopy in vineyards. Two hyperspectral indices, Gitelson-*Car*2 and Gitelson-*Anth*, sensitive to *Car* and *Anth* content, respectively, were assessed as a function of vineyard structure (LAI, crown width, row distance), physiology (C_{ab} content) and soil background effects. The inputs required for canopy simulation using the rowMCRM model were the nominal ranges for leaf optical properties, canopy layer and structure,

Author's personal copy

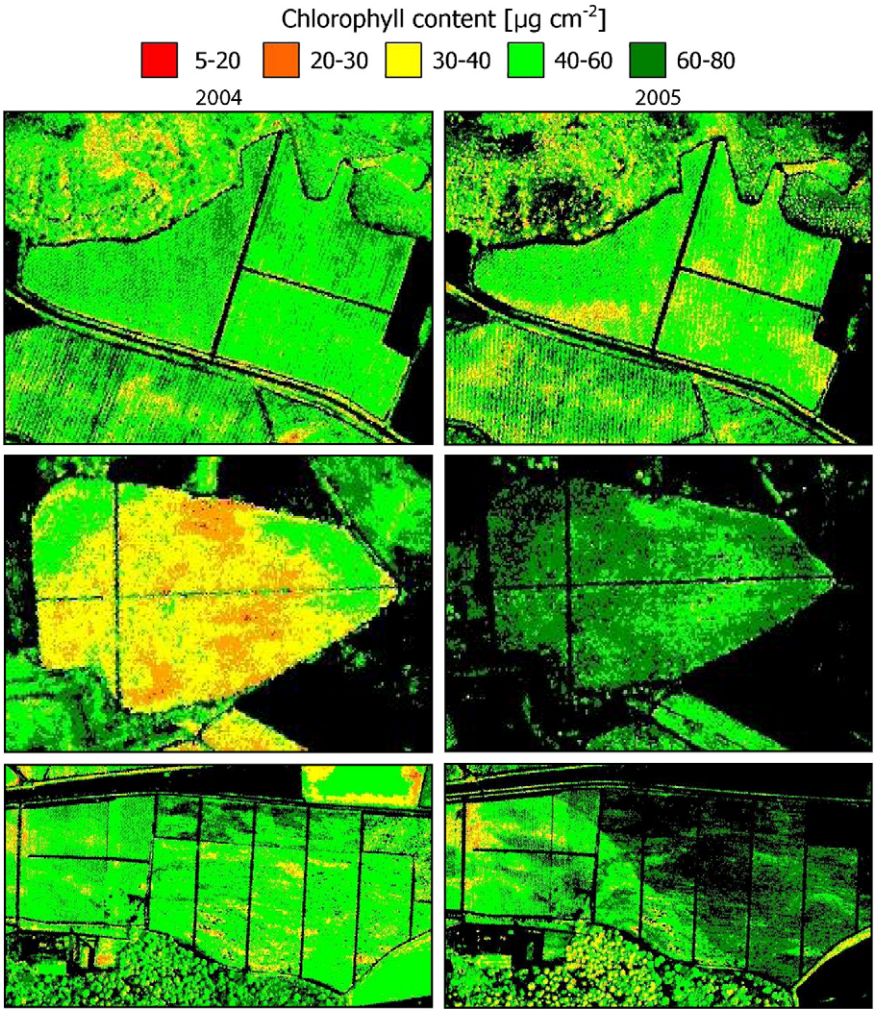

Fig. 8. Maps of spatial variation of C_{ab} content in classes of concentration ($\mu g \cdot cm^{-2}$) using the up-scaling algorithm through the TCARI/OSAVI index for the AHS 2004 (left) and 2005 (right) datasets.

and soil reflectance proposed in Zarco-Tejada et al. (2005), with the addition of row orientation effect on viewing-geometry parameters (Meggio et al., 2008).

Simulations conducted with the rowMCRM canopy reflectance model aimed at enhancing both the inter- and within-field structural and physiological variability to understand the behavior of such physiological indices in row-structured canopy conditions. In particular, different ranges of the most critical rowMCRM input parameters affecting field variability were assessed, such as row-LAI, crown width (C_w), visible soil strip (V_s), leaf chlorophyll content (C_{ab}) and soil background (ρ_s) on the Gitelson-*Car*2 and Gitelson-*Anth* indices. Mean vine dimensions in terms of C_w (0.6, 1.3 m) and V_s (1.7, 2.3 m) were used for all simulations.

The effects on *Car* (Gitelson-*Car*2, Fig. 3) and *Anth* (Gitelson-*Anth*, Fig. 4) indices as a function of different leaf C_{ab} content showed the effects in vine row LAI (1–5) and V_s length (1.7, 2.3 m), different ranges of C_w (0.6, 1.3 m) and ρ_s conditions (bright, dark). In particular, in both figures it can be successfully discriminated the main drivers of the inter- and within-variability affecting *Car* and *Anth* indices sensitivity to C_{ab} content variations: LAI, V_s, C_w and ρ_s. While vine row LAI and V_s variations have been reported in each single plot (a, b, c, d) presented in Figs. 3 and 4, C_w (a→b) and ρ_s (a→c) effects have been divided in order to determine the main drivers of variation. The Gitelson-*Car*2 index appeared highly affected by ρ_s changes (from bright to dark ρ_s) in all the different conditions tested, while row LAI was demonstrated to affect only at LAI>2 (Fig. 3). Crown structural parameters C_w and V_s showed a lower effect, with ρ_s as a main driver of variation (a→d). The Gitelson-*Car2* index appeared sensitive to C_{ab} variations only in high row LAI conditions (LAI>2), where plant structural variations also appeared to be important. The Gitelson-*Anth* index showed a similar response to the same simulations conducted for the *Car* index, confirming the higher sensitivity of C_{ab} content as a function of ρ_s (Fig. 4). In addition, the Gitelson-*Anth* index appeared more affected by C_{ab} content than the *Car* index and less affected by LAI and ρ_s at low C_{ab} content, increasing with a further change in C_{ab}.

Therefore, the effects of soil background on the physiological indices were assessed, showing the large effects due to ρ_s on the *Car* (Gitelson-*Car*2) and *Anth* (Gitelson-*Anth*) indices as a function of different C_{ab} levels (Fig. 5). A range of 3 different ρ_s spectra from bright to dark collected in the field over the same area were tested in simulations for different row LAI (1–5) in 2 opposite structural conditions in terms of V_s and C_w. These simulations assessed the high effect of ρ_s on both physiological indices as a function of C_{ab} content, with a greater effect represented by a higher vine crown dimension ($C_w = 1.3$ m) and therefore a lower visible soil strip ($V_s = 1.7$ m) conditions.

The wide range simulation results presented in Figs. 3–5 underlined that *Car* (Gitelson-*Car*2) and *Anth* (Gitelson-*Anth*) indices are

Author's personal copy

Table 3
Coefficients of determination (r^2) found for linear relationships between hyperspectral indices and grapevine structural parameters in 2004 and 2005 ($p<0.05$).

Index-ID	Reference	Grapevine structural and management parameters							
		ESA		LAI		Yield		Pruning weight	
		04	05	04	05	04	05	04	05
Leaf area index									
NDVI	Rouse et al. (1974)		0.62+						0.44+
Chlorophyll									
TCARI/OSAVI	Haboudane et al. (2002)								0.70+
Gitelson-*Chl*1	Gitelson et al. (2003, 2006)		0.60+						
Gitelson-*Chl*2	Gitelson et al. (2003, 2006)								0.51+
Carotenoid									
Chappelle-*Car*	Chappelle et al. (1992)			0.47−					
Blackburn-*Car*1	Blackburn (1998)			0.46−					
Blackburn-*Car*2	Blackburn (1998)		0.41+	0.48−					
SIPI	Peñuelas et al. (1995)			0.41−					
Gitelson-*Car*1	Gitelson et al. (2003, 2006)						0.55−		
Gitelson-*Car*2	Gitelson et al. (2003, 2006)						0.58−		
Anthocyanin									
Gamon-*Anth*	Gamon and Surfus (1999)								0.65−
Gitelson-*Anth*	Gitelson et al. (2003, 2006)					0.44−	0.55+		

ESA = Exposed Canopy Surface Area; LAI = Leaf Area Index.

affected by structure (C_w, V_s) and soil background (ρ_s). New simulations were conducted with rowMCRM to assess the expected real field variability, considering the actual range for C_{ab} (20–40 $\mu g \cdot cm^{-2}$), C_w (0.6–1.4 m in 0.2 m steps), V_s (1.6–2.4 m in 0.2 m steps) and ρ_s (bright, dark). The effect on *Car* and *Anth* indices as a function of V_s dimensions was studied for different C_w, ρ_s and C_{ab} conditions to assess the expected real field variability (Fig. 6). Simulations conducted revealed the sensitivity of Gitelson-*Car*2 (Fig. 6a,b) and Gitelson-*Anth* (Fig. 6c,d) as a function of V_s to ρ_s in both low (20 $\mu g \cdot cm^{-2}$) to medium (40 $\mu g \cdot cm^{-2}$) C_{ab} content. Fig. 6c, d underlines that the higher sensitivity of the *Anth* index to C_{ab} variations is due mainly to ρ_s. The modeling study demonstrated the influence of structure on physiological indices used for *Car* and *Anth* assessment. *Scaling-up* relationships for C_{ab} estimation and results on the assessment of the physiological indices used for grape quality estimation are described in the following section.

3. Results

3.1. Chlorosis detection using rowMCRM modeling with the AHS airborne imager

Previous field campaigns conducted in 2003 over the same study sites using the rowMCRM simulation methodology demonstrated the capability of the CASI hyperspectral airborne sensor for C_{ab} estimation in row-structured canopies (Zarco-Tejada et al., 2005; Meggio et al., 2008). Results obtained following the same methodology on the AHS sensor bandset are presented. The predictive relationship developed

Table 4
Coefficients of determination (r^2) found for linear relationships between hyperspectral indices and must composition parameters in 2004 and 2005 ($p<0.05$).

Index-ID	Reference	Must composition parameters													
		W100		°BRIX		TA		pH		TPI		Tartaric		Malic	
		04	05	04	05	04	05	04	05	04	05	04	05	04	05
Leaf area index															
NDVI	Rouse et al. (1974)			0.50+						0.62+					
Chlorophyll															
TCARI/OSAVI	Haboudane et al. (2002)			0.50−									0.53−		
Gitelson-*Chl*1	Gitelson et al. (2003, 2006)		0.65+	0.52+						0.62+					
Gitelson-*Chl*2	Gitelson et al. (2003, 2006)			0.53+						0.60+					
Carotenoid															
Chappelle-*Car*	Chappelle et al. (1992)	0.49+	0.49+	0.47−						0.59+					0.47−
Blackburn-*Car*1	Blackburn (1998)	0.49+	0.50+	0.48+						0.57+					0.44−
Blackburn-*Car*2	Blackburn (1998)	0.52+	0.48+	0.43+			0.44+			0.57+					0.47−
SIPI	Peñuelas et al. (1995)		0.63+	0.50+						0.62+					
Gitelson-*Car*1	Gitelson et al. (2003, 2006)					0.51+			0.63−			0.45+			0.81−
Gitelson-*Car*2	Gitelson et al. (2003, 2006)								0.65−						0.78−
Anthocyanin															
Gamon-*Anth*	Gamon and Surfus (1999)			0.48−					0.70−	0.53−					0.67−
Gitelson-*Anth*	Gitelson et al. (2003, 2006)			0.46−					0.66−						0.78−

W100: 100 berries weight; TA: Total Acidity; TPI: Total Polyphenol Index; Tartaric Tartaric acid content; Malic Malic acid content.

Author's personal copy

Table 5
Coefficients of determination (r^2) found for linear relationships between hyperspectral indices and color intensity (CI), hue and CIELAB coordinates for must ($p<0.05$).

Index-ID	Reference	Must color parameters (2004)						
		L	*a**	*b**	*c**	H	CI	Hue
Leaf area index								
NDVI	Rouse et al. (1974)	0.69−	0.68+		0.72+	0.73−		
Chlorophyll								
TCARI/OSAVI	Haboudane et al. (2002)	0.68−						
Gitelson-*Chl*1	Gitelson et al. (2003, 2006)	0.74−	0.74+		0.81+	0.70−		
Gitelson-*Chl*2	Gitelson et al. (2003, 2006)	0.71−	0.71+		0.75+	0.74−		
Carotenoid								
Chappelle-*Car*	Chappelle et al. (1992)	0.68−	0.7+		0.80+	0.57−	0.82+	0.74−
Blackburn-*Car*1	Blackburn (1998)	0.64−	0.69+		0.80+	0.55−	0.72+	0.72−
Blackburn-*Car*2	Blackburn (1998)	0.72−	0.64+		0.74+	0.50−	0.67+	0.68−
SIPI	Peñuelas et al. (1995)		0.71+		0.78+	0.69−		0.68−
Gitelson-*Car*1	Gitelson et al. (2003, 2006)							
Gitelson-*Car*2	Gitelson et al. (2003, 2006)							
Anthocyanin								
Gamon-*Anth*	Gamon and Surfus (1999)	0.58+	0.58−	0.45+	0.59−	0.76+		
Gitelson-*Anth*	Gitelson et al. (2003, 2006)					0.64+	0.70−	0.55+

by Meggio et al. (2008) with the rowMCRM model between C_{ab} and TCARI/OSAVI were adapted for the AHS bandset.

Simulations conducted through the rowMCRM model assessed the effect of using AHS bands 571 nm and 542 nm for TCARI calculation. Leaf C_{ab} content was estimated using the predictive scaling relationship through AHS TCARI/OSAVI calculated with both bands separately, assessing the bandset effects on the root mean square error (RMSE) for C_{ab} estimation (Fig. 7). TCARI/OSAVI calculated with band 542 nm obtained an RMSE of 7.1 and 10.3 $\mu g \cdot cm^{-2}$ for the AHS 2004 and 2005 datasets confirming, in any case, the reliability of the scaling relationship (Fig. 7a). C_{ab} estimation through AHS band 571 nm for TCARI/OSAVI calculation yielded better results from both the 2004 and 2005 datasets, with an RMSE of 3.7 and 4.1 $\mu g \cdot cm^{-2}$, respectively (Fig. 7b). Results obtained suggested, therefore, the use of AHS band 571 nm for TCARI/OSAVI calculation for C_{ab} estimation, yielding an overall RMSE of 3.8 $\mu g \cdot cm^{-2}$ considering the two study years together, instead of band 542 nm, which yielded an overall RMSE of 8.6 $\mu g \cdot cm^{-2}$ (Fig. 7c).

These results demonstrate the feasibility of estimating C_{ab} with the AHS airborne sensor, an instrument with 30 nm FWHM bands, through the modeling methodology presented. The scaling algorithm for TCARI/OSAVI to estimate C_{ab} content proposed in Meggio et al. (2008), considering both before and after noon viewing geometries and differences in vine row orientation, was applied to the AHS images to obtain maps of leaf C_{ab} content for five levels, ranging from 5 to 80 $\mu g \cdot cm^{-2}$ (Fig. 8). These C_{ab} maps show the within- and inter-field variability in vineyards affected by iron deficiency chlorosis, displaying different chlorosis levels for both years.

Table 6
Coefficients of determination (r^2) found for linear relationships between hyperspectral indices and must quality indices ($p<0.05$).

Index-ID	Reference	Must quality indices							
		QI-1		QI-2		IMAD		CIRG	
		04	*05*	04	05	04	05	04	05
Leaf area index									
NDVI	Rouse et al. (1974)			0.63−					
Chlorophyll									
TCARI/OSAVI	Haboudane et al. (2002)								
Gitelson-*Chl*1	Gitelson *et al. (2003, 2006)*		0.57−	0.67+					
Gitelson-*Chl*2	Gitelson et al. (2003, 2006)			0.62+					
Carotenoid									
Chappelle-*Car*	Chappelle et al. (1992)		0.53−	0.68+			0.44−		0.50−
Blackburn-*Car*1	Blackburn (1998)		0.54−	0.70+			0.44−		0.48−
Blackburn-*Car*2	Blackburn (1998)		0.55−	0.68+			0.48−		0.51−
SIPI	Peñuelas et al. (1995)		0.58−	0.65+					
Gitelson-*Car*1	Gitelson et al. (2003, 2006)	0.48−				0.59−	0.42−	0.45−	0.92−
Gitelson-*Car*2	Gitelson et al. (2003, 2006)					0.71−	0.42−	0.68−	0.93−
Anthocyanin									
Gamon-*Anth*	Gamon and Surfus (1999)			0.54−				0.43−	0.64−
Gitelson-*Anth*	Gitelson et al. (2003, 2006)						0.48−	0.56−	0.94−

%vol: probable alcoholic degree.
QI-1: %vol/100 berries weight; QI-2: $(TPI/40)^2 \times (\%vol - 10)$; CIRG: $(180 - H^*)/(L^* + C^*)$; IMAD: °Brix/TA.

Author's personal copy

Table 7
Coefficients of determination (r^2) found for linear relationships between hyperspectral indices and berry skins composition ($p<0.05$).

Index-ID	Reference	Skin extracts components and quality parameters (2005)						
		W100 Skins	DMACH Index	Tannins	Catechins	AT	PT	CIRG
Leaf area index								
NDVI	Rouse et al. (1974)		0.72−					
Chlorophyll								
TCARI/OSAVI	Haboudane et al. (2002)							
Gitelson-*Chl*1	Gitelson et al. (2003, 2006)	0.53+	0.50−		0.51−		0.47−	
Gitelson-*Chl*2	Gitelson et al. (2003, 2006)		0.67−					
Carotenoid								
Chappelle-*Car*	Chappelle et al. (1992)	0.50+			0.57−	0.66−	0.63−	0.70−
Blackburn-*Car*1	Blackburn (1998)	0.52+			0.58−	0.61−	0.62−	0.70−
Blackburn-*Car*2	Blackburn (1998)	0.48+			0.55−	0.67−	0.62−	0.66−
SIPI	Peñuelas et al. (1995)	0.51+	0.60−		0.50−		0.58−	
Gitelson-*Car*1	Gitelson et al. (2003, 2006)			0.44−		0.75−	0.48−	0.68−
Gitelson-*Car*2	Gitelson et al. (2003, 2006)			0.48−		0.75−	0.47−	0.68−
Anthocyanin								
Gamon-*Anth*	Gamon and Surfus (1999)			0.59−		0.44−		0.45−
Gitelson-*Anth*	Gitelson et al. (2003, 2006)			0.52−		0.71−	0.48−	0.68−

W100 skins: 100 skins weight; Tannins: Total Tannins content; AT: Total Anths content; PT: Total Polyphenols content.

3.2. Relationships between hyperspectral indices and physiological data for grape quality assessment

Physiological measurements conducted for two years on grapes sampled one week before harvest were used to assess the relationship with hyperspectral indices sensitive to pigment content (C_{ab}, *Car*, and *Anth*). Coefficients of determination (r^2) found for linear regression relationships between hyperspectral indices calculated from AHS imagery and grape and must quality parameters were obtained for four types of indices: leaf area index and structural indices (i), C_{ab} (ii), *Car* (iii) and *Anth* content (iv). Coefficients of determination values resulting from linear regression are presented in Tables 3–7, along with the direct/inverse relationship (+ or −). The relationships with $r^2<0.4$ and $p>0.05$ are not included in the tables (relationships with $r^2>0.6$ are underlined in bold).

Plant structural and management parameters (LAI, exposed canopy surface area (ESA), yield and pruning weight) were related to vegetation indices (Table 3). Linear relationships were obtained between hyperspectral indices generally considered sensitive to vegetative vigor and grapevine structural parameters. In particular, TCARI/OSAVI and NDVI vegetation indices yielded coefficients of determination with pruning weight ($r^2=0.7$) and exposed canopy surface ($r^2=0.62$), respectively. Mean mineral concentrations in petioles were similar or higher than reference values for Ribera del Duero *Appellation d'Origine* (González and Martín, 2006). However, there were wide ranges of variation within samples for Mn, Cu and Zn (data not shown), including some study subzones with deficiencies in these micronutrients. Significant correlations between Zn foliar content and yield and vigor of vineyards in the same study area have been reported previously (Martín et al., 2008).

Relationships with must composition parameters (°BRIX, pH, total acidity (TA), tartaric and malic acid content) are shown in Table 4, displaying those obtained with the hyperspectral indices tested in this study. While the traditional NDVI index yielded relationships with °BRIX ($r^2=0.5$) and the Total Polyphenol Index — TPI ($r^2=0.62$), other physiological indices, Gamon-*Anth* and Gitelson-*Car*1, yielded significant linear relationships with pH ($r^2=0.7$) and malic acid content ($r^2=0.81$), respectively. Coefficients of determination obtained for chromatic characteristics of must (Table 5) show that physiological indices appeared more suitable for color intensity (CI) and hue estimation than traditional vegetation indices. Linear relationships performed resulted in high coefficients of determination with CI ($r^2=0.82$, 0.72, 0.70) and hue ($r^2=0.74$, 0.72, 0.55) for the Chappelle-*Car*, Blackburn-*Car*1 and Gitelson-*Anth* physiological indices, respectively. Different must quality indices, such as IMAD (°Brix/TA) and the Chromatic Index for Red Grapes (CIRG) (Table 6), show consistent results obtained for both seasons, 2004 and 2005. In particular, unlike the results achieved with traditional (NDVI) and more innovative (TCARI/OSAVI) indices sensitive to vegetative vigor and C_{ab} content, physiological indices sensitive to *Car* and *Anth* content appeared more suitable for grape quality assessment in the vineyards studied. Specifically, the inverse linear relationships

Table 8
Hyperspectral indices with the highest coefficients of determination for each grapevine quality parameter.

Must composition		Must quality	
W100	Gitelson-*Chl*1 SIPI	QI-1	SIPI Gitelson-*Chl*1
°BRIX	Gitelson-*Chl*1-2	QI-2	Blackburn-*Car*1-2 Chappelle-*Car*
pH	Gamon-*Anth* Gitelson-*Anth*	IMAD	Gitelson-*Car*1-2
TPI	Gitelson-*Chl*1 SIPI	CIRG	Gitelson-*Anth* Gitelson-*Car*1-2
Malic	Gitelson-*Car*1-2 Gitelson-*Anth*		
Must color		**Skin extracts components and quality**	
L	Gitelson-*Chl*1 Blackburn-*Car*2	W100 skins	Gitelson-*Chl*1 Blackburn-*Car*1
*a**	Gitelson-*Chl*1-2 SIPI	DMACH index	Gitelson-*Chl*2
*c**	Gitelson-*Chl*1 Chappelle-*Car* Blackburn-*Car*1	Tannins	Gamon-*Anth*
H	Gamon-*Anth* Gitelson-*Chl*2	Catechins	Chappelle-*Car* Blackburn-*Car*1
CI	Chappelle-*Car* Blackburn-*Car*1	AT	Gitelson-*Car*1-2 Gitelson-*Anth*
Hue	Chappelle-*Car* Blackburn-*Car*1	PT	Chappelle-*Car* Blackburn-*Car*1-2
		CIRG	*Chappelle-Car* *Blackburn-Car1* Gitelson-*Car*1-2 Gitelson-*Anth*

Author's personal copy

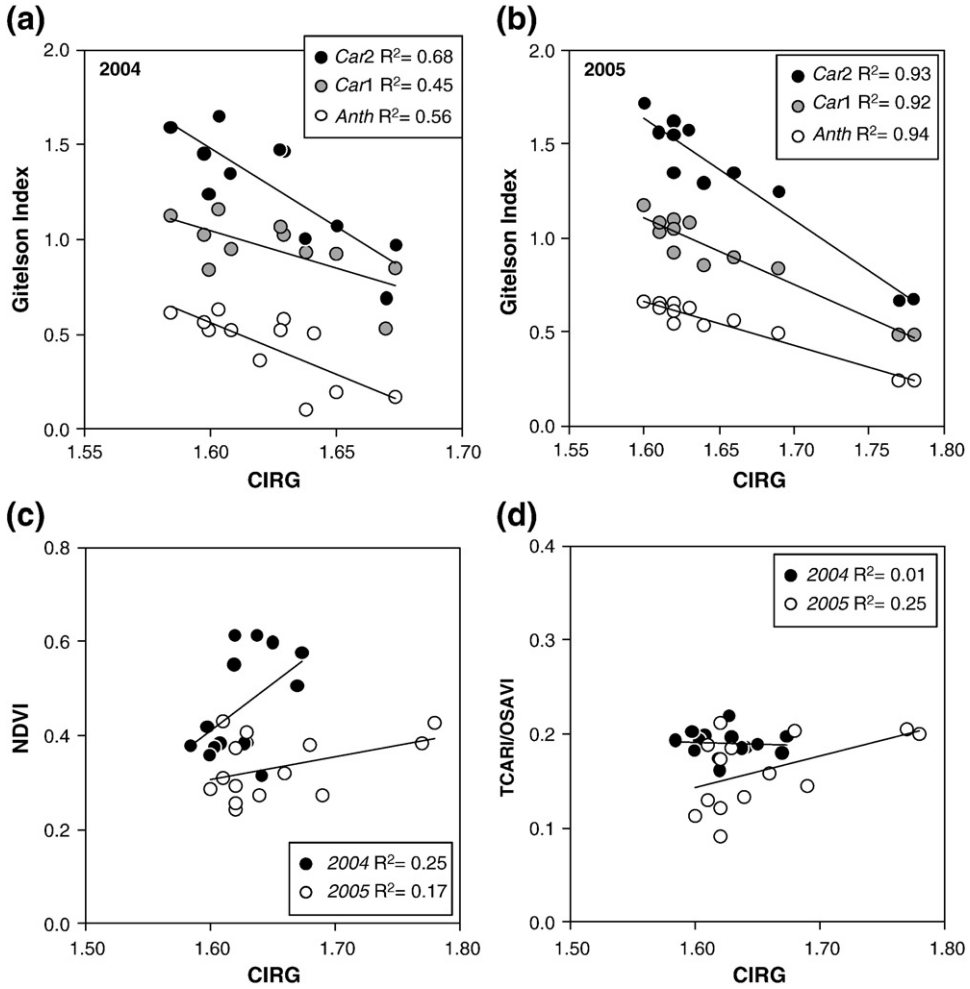

Fig. 9. Relationships between the must Chromatic Index for Red Grapes (CIRG) and physiological indices sensitive to *Car* and *Anth* pigment content (a,b) and traditional indices sensitive to C_{ab} content (c,d).

obtained between CIRG and the physiological indices yielded consistent coefficients of determination, $r^2 = 0.68$ (2004) and $r^2 = 0.93$ (2005) for Gitelson-*Car*2, and $r^2 = 0.56$ (2004) and $r^2 = 0.94$ (2005) for the Gitelson-*Anth* index. The IMAD quality index yielded interesting linear relationships with the Gitelson-*Car*2 physiological index, obtaining $r^2 = 0.71$ and $r^2 = 0.42$ for the 2004 and 2005 season datasets, respectively. The Gitelson-*Car2* and Gitelson-*Anth* indices were inversely correlated with B foliar levels in 2004 (Pearson's $r = -0.89$, $p<0.01$) and with K, Cu, Zn and B foliar levels in 2005 (r values from -0.61 to -0.88, $p<0.05$).

Finally, results obtained for berry skin composition parameters in the 2005 field campaign (100 skins weight, DMACH index, total tannin index, total *Anth* (AT), total polyphenols (PT) and CIRG) (Table 7) show that, while the traditional NDVI vegetation index appeared well correlated ($r^2 = 0.72$) only with the DMACH index, hyperspectral indices sensitive to physiological properties were shown to be more suitable for berry skin composition estimation. In particular, indices sensitive to *Car* and *Anth* content appeared well correlated (negatively) with AT, PT and CIRG physiological parameters. Consistent relationships have been obtained between Gitelson indices and berry skin AT content: $r^2 = 0.75$ (Gitelson-*Car*) and $r^2 = 0.71$ (Gitelson-*Anth*). The berry skin PT appeared well correlated with the Chappelle-*Car* and Blackburn-*Car* indices, yielding coefficients of determination of $r^2 = 0.63$ and 0.62, respectively. The skin CIRG index for skin extracts was inversely well correlated with the Chappelle-*Car* ($r^2 = 0.7$) and Gitelson-*Anth* ($r^2 = 0.68$) physiological indices.

Positive Pearson`s coefficients between total anthocyanin concentrations in skin extracts and K ($r = 0.54$, $p<0.05$), Cu ($r = 0.69$, $p<0.01$), Zn ($r = 0.76$, $p<0{,}001$) and B ($r = 0.52$, $p<0{,}05$) content in petioles were observed. Total polyphenols also were correlated with Cu and B levels ($r = 0.75$ and $r = 0.72$, respectively, $p<0.01$). The best relationships were obtained for Zn-Gamon-*Anth* ($r = -0.91$) and B-Blackburn-*Car*2 ($r = -0.86$).

In summary, these results suggest that *traditional* vegetation indices sensitive to leaf area index (NDVI) and newer indices related to C_{ab} content (TCARI/OSAVI) yielded lower relationships than physiological indices sensitive to carotenoid *Car* and anthocyanin *Anth* content. In particular, the comparison between physiological indices potentially useful for estimating grape quality showed relationships for the two years between must and skin composition parameters and *Car* and *Anth* indices (Gitelson-*Car*1,-*Car*2 and Gitelson-*Anth* indices, Chappelle-*Car*, Blackburn-*Car*1,-*Car*2) (Table 8). The best relationships were obtained for wine grape quality parameters, as presented in Figs. 9 to 13. The relationships between the chromatic index (CIRG) and *Car*, *Anth* indices, TCARI/OSAVI and NDVI (Fig. 9) demonstrate the capability of physiological indices for grape quality assessment. While the Gitelson-*Car*2 and Gitelson-*Anth*

Author's personal copy

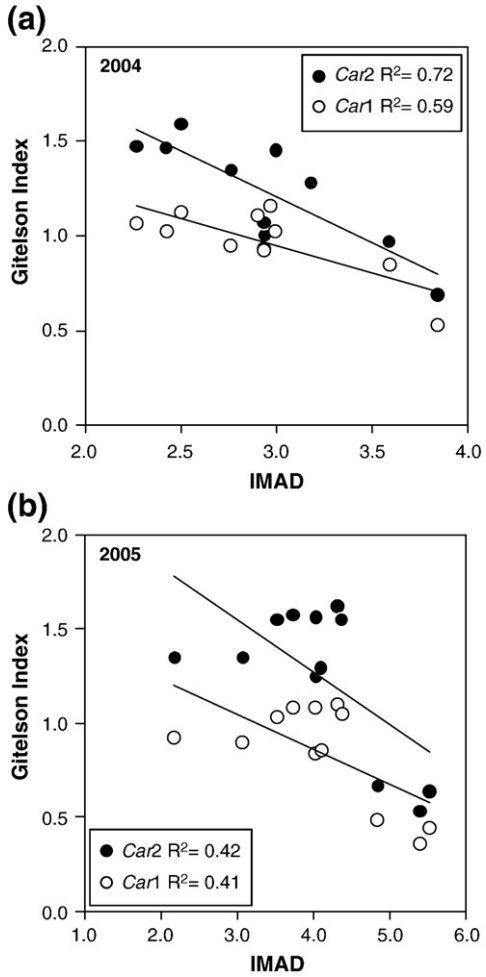

Fig. 10. Relationships between the IMAD (°vol/total acidity) Index and physiological indices sensitive to *Car* and *Anth* pigment content.

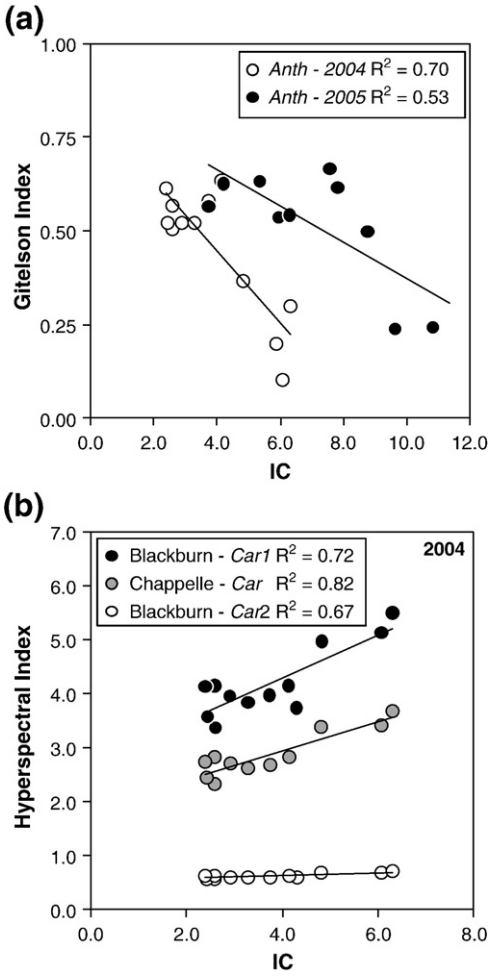

Fig. 11. Relationships between must color intensity (CI) and physiological indices sensitive to *Car* and *Anth* pigment content.

indices yielded coefficients of determination ranging between r^2 ~0.5–0.6 and r^2 ~0.9 with CIRG for the 2004 and 2005 seasons, respectively, NDVI and TCARI/OSAVI showed lower relationships ($r^2<0.25$).

The relationships between the IMAD index and Gitelson-*Car* indices (Fig. 10) yielded coefficients of determination ranging between r^2 ~0.6–0.7 and r^2 ~0.4 for the 2004 and 2005 seasons, respectively. Must color intensity (CI) obtained consistent relationships with the Gitelson-*Anth* index for both the 2004 ($r^2=0.7$) and 2005 ($r^2=0.53$) growing seasons (Fig. 11). Consistent relationships were obtained between berry skin total polyphenols (PT) collected in the 2005 season and physiological indices sensitive to *Car* content, with a coefficient of determination of r^2 ~0.6 for the Chappelle-*Car*, Blackburn-*Car*1-2 and SIPI indices (Fig. 12). The berry skin Chromatic Index for Red Grapes (CIRG) resulted in consistent relationships with both *Car* and *Anth* indices, yielding a coefficient of determination of around $r^2=0.68$–0.7 (Fig. 13).

The quantitative results obtained in Figs. 9 and 10 enabled the calculation of spatial maps of grape quality for CIRG (Fig. 14) and IMAD (Fig. 15) indices. The maps were obtained through Gitelson-*Car*2 index linear relationships with CIRG(2004) [$y=-8.252(x)+14.685$], CIRG(2005) [$y=-5.4395(x)+10.344$], IMAD(2004) [$y=-0.4898(x)+2.6772$] and IMAD(2005) [$y=-0.2788(x)+2.3851$] quality indices for three vineyard study sites, showing both the inter- and within-field variability between the different vineyards for two consecutive years.

4. Discussion

Simulations conducted with the rowMCRM model demonstrated the feasibility of estimating C_{ab} content using TCARI/OSAVI from AHS 30 nm FWHM spectral bands. Results underlined the strong effect of within- and between-field variability on the TCARI/OSAVI hyperspectral index when calculated with band 571 nm instead of band 541 nm for the TCARI index. Leaf C_{ab} content estimated from AHS TCARI/OSAVI calculated with band 571 nm through the scaling algorithm proposed by Meggio et al. (2008) provided the best results, yielding an RMSE of 3.7 and 4.1 $\mu g \cdot cm^{-2}$ for the 2004 and 2005 datasets, respectively, and resulting in an overall RMSE of 3.8 $\mu g \cdot cm^{-2}$ (RMSE = 8.6 $\mu g \cdot cm^{-2}$ if using band 542 nm). Such consistent results enabled the calculation of C_{ab} content distribution maps in 5 levels of chlorophyll concentration (5–80 $\mu g \cdot cm^{-2}$).

The rowMCRM model simulations were used to assess canopy structural effects on physiological indices sensitive to *Car* and *Anth* content as a function of the typical row-structured canopy variables in vineyards (LAI, crown width, row distance, C_{ab} content and soil background effects) and then consider the expected real field variability and actual range parameters collected in the field sites. Modeling results concluded that *Car* (Gitelson-*Car2*) and *Anth* (Gitelson-*Anth*) indices were highly affected by canopy structure (C_w, V_s) and soil background (ρ_s).

Coefficients of determination resulting from the linear regression between field parameters and physiological indices (in both years of

Author's personal copy

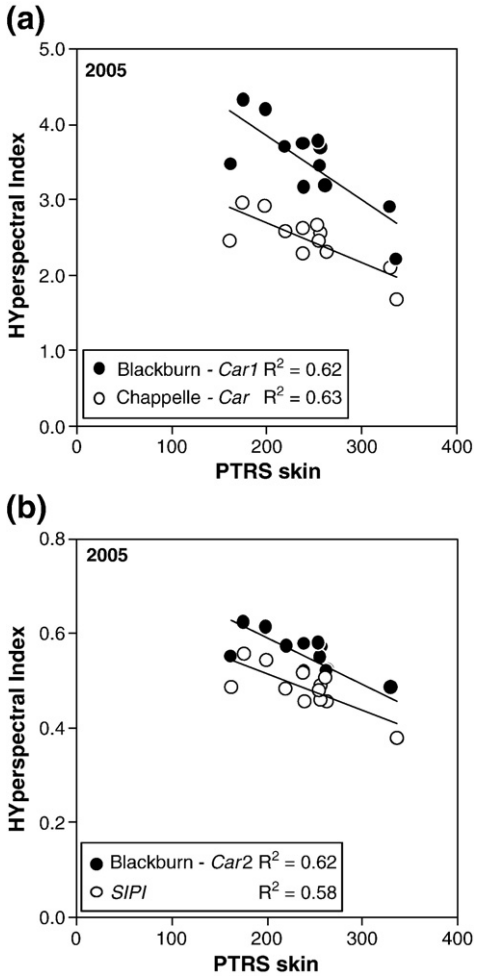

Fig. 12. Relationships between berry skin total polyphenols content and physiological indices sensitive to *Car* and *Anth* pigment content.

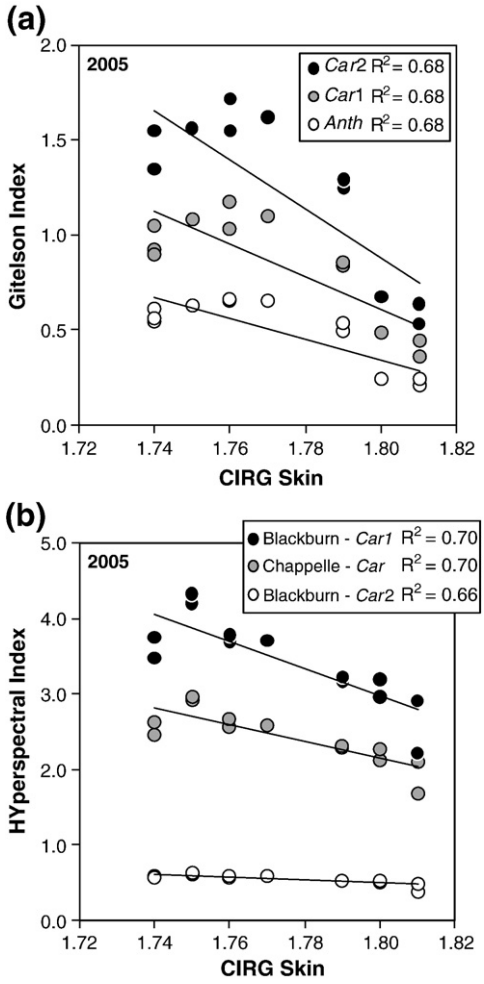

Fig. 13. Relationships between berry skin CIRG and physiological indices sensitive to *Car* and *Anth* pigment content.

the study) revealed the ability of physiological hyperspectral remote sensing indices to assess grape quality in vineyards affected by iron deficiency chlorosis, showing superior results compared to traditional vegetation indices. In particular, and despite their extensive use in remote sensing studies, NDVI and TCARI/OSAVI, utilized for vegetative vigor and leaf chlorophyll content retrieval, respectively, showed low coefficients of determination for physiological parameters linked to grape quality. In addition, results obtained from physiological indices sensitive to *Car* and *Anth* content underlined their potential for grape quality assessment, particularly phenolic composition and chromatic features of grapes (Table 8). Consistent results were obtained for the CIRG index, yielding coefficients of determination of $r^2 = 0.68$ (Gitelson *Car*2 index) and $r^2 = 0.56$ (Gitelson-*Anth* index) for the 2004 dataset, and $r^2 = 0.93$ (Gitelson-*Car*2 index) and $r^2 = 0.94$ (Gitelson-*Anth* index) for the 2005 dataset. Further results showed the Gitelson-*Car*2 index capability for IMAD quality index estimation with coefficients of determination of $r^2 = 0.72$ and 0.42 for the 2004 and 2005 datasets, respectively. In addition, berry skin quality parameters such as total polyphenol content (PT) and the CIRG index were well estimated through physiological indices, obtaining consistent relationships: $r^2 = 0.63$ (Chappelle-*Car* index) and $r^2 = 0.7$ (Blackburn-*Car*1 index) for PT and CIRG, respectively.

Phenolic compounds, anthocyanins and tannins are responsible for the color and astringency of red wines (Ribéreau-Gayon & Glories, 1987). Berry skin phenolic composition and color play a key role in quality determination for grapes such as Tempranillo. In addition, the phenolic potential of grapes is of great importance in the Ribera del Duero *Apellation d'Origine* area, where other technologic quality parameters (sugar content, acidity, etc.) are not considered limiting factors for winemaking. In vineyards affected by iron chlorosis, the lack of photosynthetic pigments in leaves is a major factor limiting grape ripening. Previous work over the same area monitored in this study (Martín et al., 2007) reported that differences in grape quality parameters can be predicted by differences in leaf chlorophyll content of vines. The most obvious characteristic of the leaves from iron deficient plants is chlorosis, due to low concentration per area of chlorophylls and carotenoids. However, not all photosynthetic pigments are decreased to the same extent by iron deficiency, xanthophylls being less affected than chlorophylls and β-carotene (Abadia et al., 1999; Bertamini et al., 2001; Morales et al., 1994). On the other hand, an increase in leaf anthocyanin contents may reflect different biotic and abiotic stresses in plants, including mineral deficiencies (Chalker-Scott, 1999; Harbone, 1976).

The strong negative relationships reported between physiological indices based on *Anth* and *Car* with phenolic potential parameters, where relationships with indices based on chlorophyll content were not significant (Tables 6 and 7), suggest that an increase in the red component of color (derived from carotene and anthocyanin) in leaves in summer could be a better indicator than chlorosis to detect difficulties in phenolic ripening for vines affected by iron deficiency chlorosis.

Author's personal copy

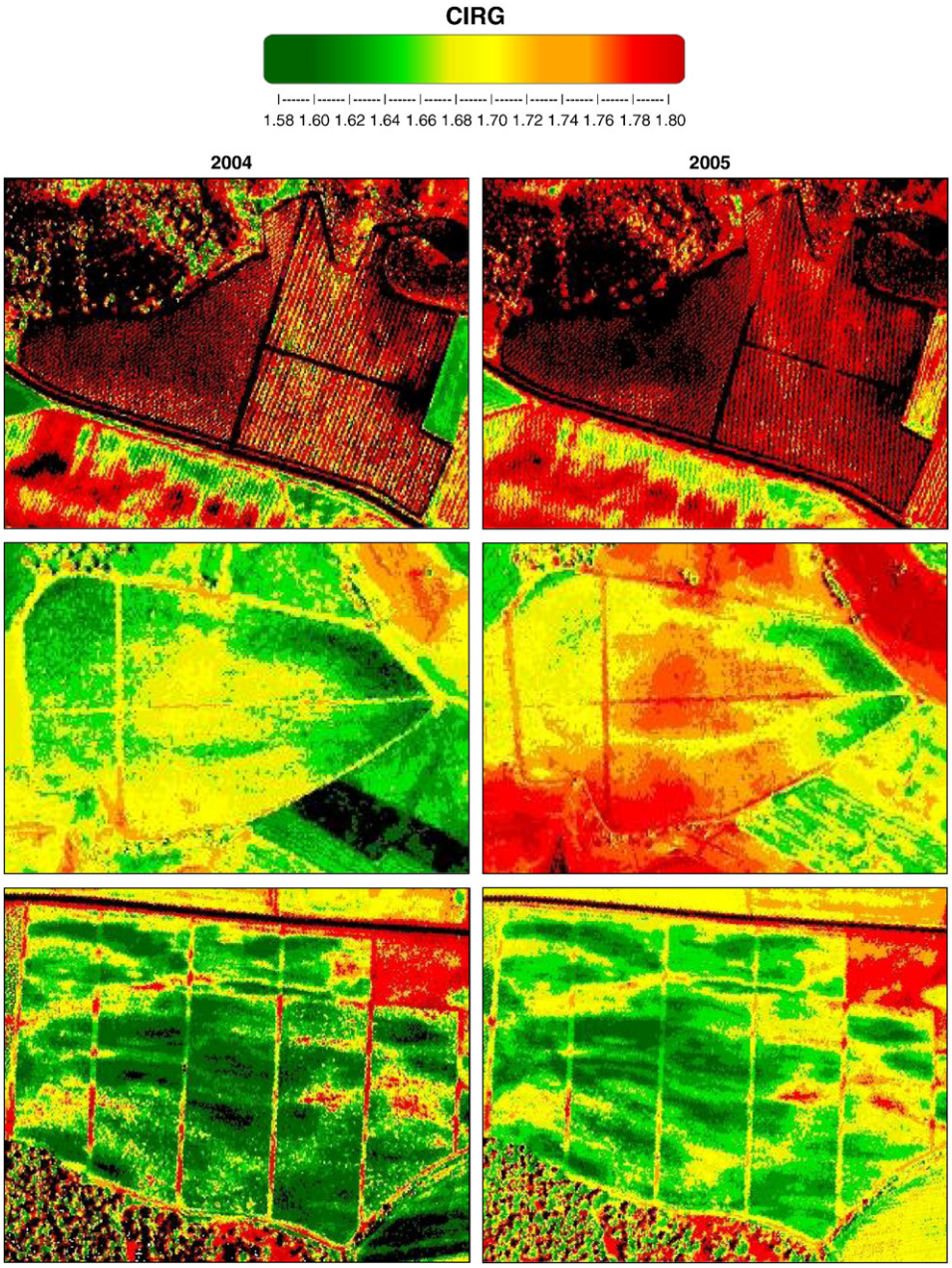

Fig. 14. Maps of Chromatic Index for Red Grapes (CIRG) obtained through the relationship with the Gitelson-*Car*2 physiological index for the 2004 and 2005 growing seasons.

Physicochemical conditions in calcareous soils, such as high pH, decrease the assimilation of micronutrients such as Cu and Zn, as well as iron (Martín et al., 2008). Our study showed significant relationships between K, Cu, Zn and B petiole levels with polyphenol contents in grapes and with *Car* and *Anth* physiological remote sensing indices. Therefore, these physiological spectral indices could be useful to detect nutritional effects related to iron deficiency affecting grape phenolic ripening.

5. Conclusions

This study suggests the potential of physiological remote sensing indices related to carotene and anthocyanin pigments content in leaves as grape quality indicators in vineyards affected by iron chlorosis, using high-resolution hyperspectral imagery. These indices could be used, as an alternative to others based on C_{ab} foliar content, to monitor iron and other concurrent micronutrient deficiencies in vines before veraison, predicting the potential grape quality at harvest. The generation of quality maps from hyperspectral remote sensing would help assess within- and inter-field ripening variability by proposing spatially segmented harvesting zones for optimum winemaking.

Acknowledgements

This work was supported by AGL2009-13105-C03-01 grants from the Ministerio de Ciencia e Innovación (MICINN), and VA016B05 grant from the Junta de Castilla y León (Spain). The authors are grateful to the Consejo Regulador de la Denominación de Origen Ribera de Duero, Bodegas Monasterio S.L. and Fertiberia S.A. for their collaboration in conducting this research. F. Meggio is supported by the FISR project

Author's personal copy

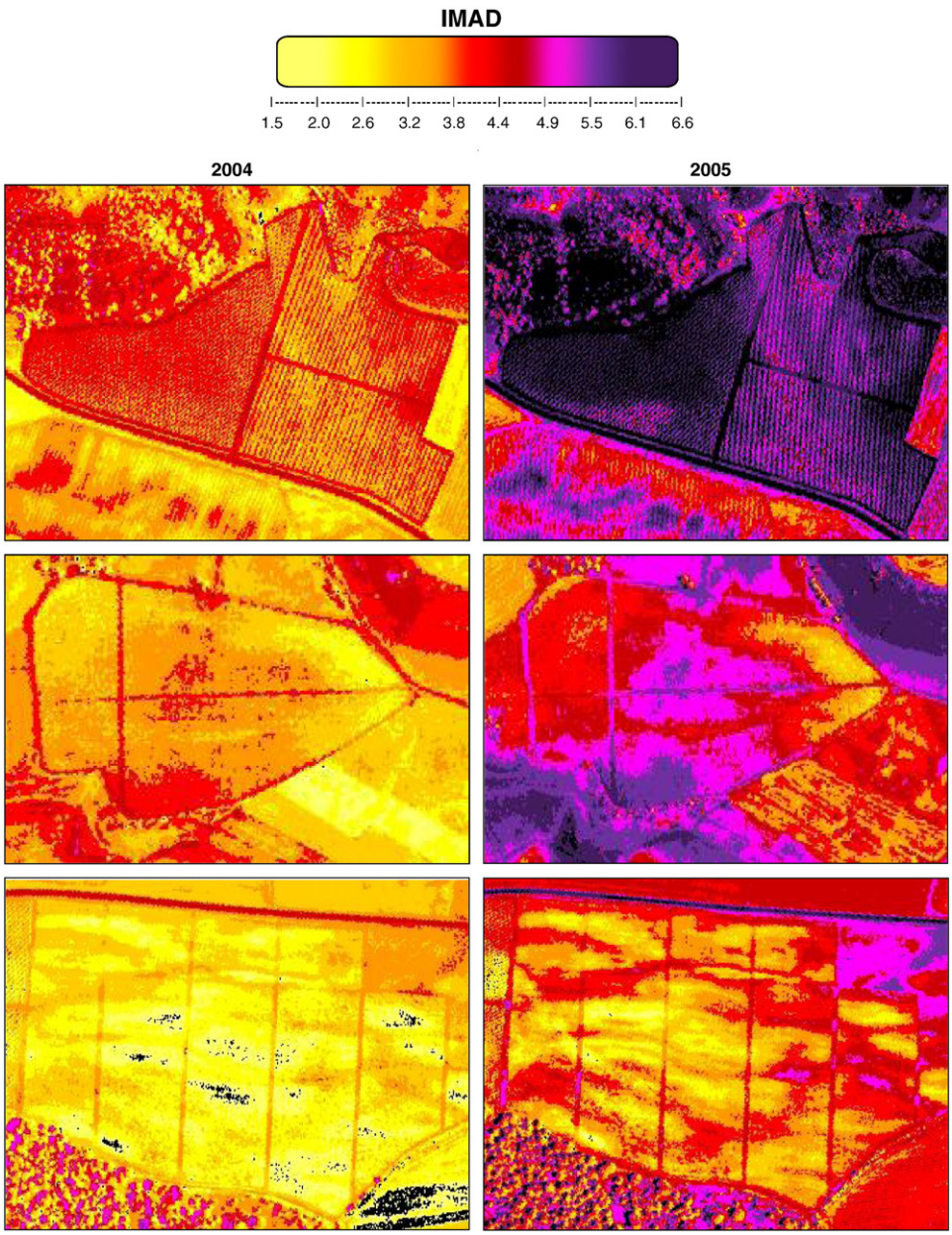

Fig. 15. Maps of IMAD (°Vol/total acidity) obtained through the relationship with the Gitelson-*Car*2 physiological index for the 2004 and 2005 growing seasons.

Carboitaly and gratefully acknowledges the financial support from Gini Foundation.

References

Abadía, J., Morales, F., & Abadía, A. (1999). Photosystem II efficiency in low chlorophyll, iron-deficient leaves. *Plant and Soil*, *215*, 183—192.

Bate-Smith, E. C. (1954). Astringency in foods. *Food*, *23*, 124.

Ben-Dor, E., & Levin, N. (2000). Determination of surface reflectance from raw hyperspectral data without simultaneous ground data measurements: a case study of the GER 63-channel sensor data acquired over Naan, Israel. *International Journal of Remote Sensing*, *21*, 2053—2074.

Bertamini, M., Nedunchezhian, N., & Borghi, B. (2001). Effect of iron deficiency induced changes on photosynthetic pigments, ribulose-1, 5-bisphosphate carboxylase, and photosystem activities in field grown grapevine (Vitis vinifera L. cv. Pinot noir) leaves. *Photosynthetica*, *39*(1), 59—65.

Blackburn, G. A. (1998). Quantifying chlorophylls and carotenoids at leaf and canopy scales: An evaluation of some hyperspectral approaches. *Remote Sensing of the Environment*, *66*, 273—285.

Carbonneau, A. (1995). La surface foliaire exposeé potentielle. *Progrés Agricole et Viticole*, *112*, 204—212.

Carreño, J., Martínez, A., Almela, L., & Fernández-López, J. A. (1995). Proposal of an index for the objective evaluation of the colour of red table grapes. *Food Research International*, *28*, 373—381.

Carter, G. A. (1994). Ratios of leaf reflectances in narrow wavebands as indicators of plant stress. *International Journal of Remote Sensing*, *15*, 697—704.

Carter, G. A., & Spiering, B. A. (2002). Optical properties of intact leaves for estimating chlorophyll concentration. *Journal of Environmental Quality*, *31*(5), 1424—1432.

Castino, M., Ubigli, M., Corino, L., Luzzati, A., Siragusa, N., & Nappi, P. (1987). *Oenological effects of nutrients deficiencies on the grape variety Barbera cultivated in Piedmont vineyards, vol. 14.* (pp. 37—54)Bologna: Vignevini.

Chalker-Scott, L. (1999). Environmental significance of anthocyanins in plan stress responses. *Photochemistry and Photobiology*, *70*, 1—9.

Chappelle, E. W., Kim, M. S., & McMurtrey, J. E., III (1992). Ratio analysis of reflectance spectra (RARS): An algorithm for the remote estimation of the concentrations of chlorophyll a, chlorophyll b, and carotenoids in soybean leaves. *Remote Sensing of Environment*, *39*, 239—247.

Chen, Y., & Barak, P. (1982). Iron nutrition in calcareous soils. *Advances in Agronomy*, *35*, 217—240.

CIE. (1986). *Colorimetry*, 2nd edition . Vienna: C.I.E.

Daughtry, C. S. T., Walthall, C. L., Kim, M. S., Brown de Colstoun, E., & McMurtrey, J. E. I. I. I. (2000). Estimating corn leaf chlorophyll concentration from leaf and canopy reflectance. *Remote Sensing of Environment*, *74*, 229—239.

Dawson, T. P., Curran, P. J., & Plummer, S. E. (1998). LIBERTY — modeling the effects of leaf biochemical concentration on reflectance spectra. *Remote Sensing of Environment*, *65*, 50—60.

Dobrowski, S. Z., Ustin, S. L., & Wolpert, J. A. (2002). Remote estimation of vine canopy density in vertically shoot-positioned vineyards: determining optimal vegetation indices. *Australian Journal of Grape and Wine Research*, *8*(2), 117—125.

Author's personal copy

Dobrowski, S. Z., Ustin, S. L., & Wolpert, J. A. (2003). Grapevine dormant pruning weight prediction using remotely sensed data. *Australian Journal of Grape and Wine Research*, *9*(3), 177−182.

European Commission. (1990). Regulation (EEC) Nº 2676/90 of 17 September (1990) community methods for the analysis of wines.*Official Journal of the European Communities*, *L272*, 0001−0192 3 October 1990.

Fernández-Escobar, R., Moreno, R., & García-Creus, M. (1999). Seasonal changes of mineral nutrients in olive leaves during the alternate-bearing cycle. *Scientia Horticulturae*, *82*, 24−45.

Fuentes, D. A., Gamon, J. A., Qiu, H., Sims, D. A., & Roberts, D. A. (2001). Mapping Canadian boreal forest vegetation using pigment and water absorption features derived from AVIRIS sensor. *Journal of Geophysical Research*, *106*, 33565−33577.

Gamon, J. A., & Surfus, J. S. (1999). Assessing leaf pigment content and activity with a reflectometer. *New Phytologist*, *143*, 105−117.

Gamon, J. A., Peñuelas, J., & Field, C. B. (1992). A narrow-wave band spectral index that track diurnal changes in photosynthetic efficiency. *Remote Sensing of Environment*, *41*, 35−44.

García-Barceló, J. (1990). Compuestos fenólicos. *Técnicas Analíticas para Vinos* (pp. 8.3−8.33). Moja-Olérdola: G.A.B.

Gitelson, A. A., & Merzlyak, M. N. (1996). Signature analysis of leaf reflectance spectra: Algorithm development for remote sensing of chlorophyll. *Journal of Plant Physiology*, *148*, 494−500.

Gitelson, A. A., Merzlyak, M. N., & Lichtenthaler, H. (1996). Detection of red edge position and chlorophyll content by reflectance measurements near 700 nm. *Journal of Plant Physiology*, *148*, 501−508.

Gitelson, A. A., Merzlyak, M. N., & Chivkunova, O. B. (2001). Optical properties and non-destructive estimation of anthocyanin content in plant leaves. *Journal of Photochemistry and Photobiology B-Biology*, *74*, 38−45.

Gitelson, A. A., Zur, Y., Chivkunova, O. B., & Merzlyak, M. N. (2002). Assessing carotenoid content in plant leaves with reflectance spectroscopy. *Journal of Photochemistry and Photobiology B-Biology*, *75*, 272−281.

Gitelson, A. A., Gritz, U., & Merzlyak, M. N. (2003). Relationships between leaf chlorophyll content and spectral reflectance and algorithms for non-destructive chlorophyll assessment in higher plant leaves. *Journal of Plant Physiology*, *160*, 271−282.

Gitelson, A. A., Keydan, G. P., & Merzlyak, M. N. (2006). Three-band model for noninvasive estimation of chlorophyll, carotenoids, and anthocyanin content in higher plant leaves. *Geophysical Research Letters*, *33*, L11402, doi:10.1029/2006GL026457

González, M. R., & Martín, P. (2006). Niveles de referencia para el diagnóstico nutricional del viñedo en la Ribera del Duero. *Vida Rural*, *226*, 44−47.

Gueymard, C.A. (1995). SMARTS, A Simple Model of the Atmospheric Radiative Transfer of Sunshine: Algorithms and Performance Assessment. Technical Report No. FSEC-PF-270-95. Cocoa, FL: Florida Solar Energy Center.

Haboudane, D., Miller, J. R., Tremblay, N., Zarco-Tejada, P. J., & Dextraze, L. (2002). Integrated narrow-band vegetation indices for prediction of crop chlorophyll content for application to precision agriculture. *Remote Sensing of Environment*, *81*, 416−426.

Hall, A., Lamb, D. W., Holzapfel, B., & Louis, J. (2002). Optical remote sensing applications in viticulture — A review. *Australian Journal of Grape and Wine Research*, *8*(1), 36−47.

Hall, A., Louis, J., & Lamb, D. W. (2003). Characterising and mapping vineyard canopy using high-spatial-resolution aerial multispectral images. *Computers & Geosciences*, *29*(7), 813−822.

Hall, A., Louis, J. P., & Lamb, D. W. (2008). Low-resolution remotely sensed images of winegrape vineyards map spatial variability in planimetric canopy area instead of leaf area index. *Australian Journal of Grape and Wine Research*, *14*(1), 9−17.

Harbone, K. B. (1976). Function of flavonoids in plants. In T. W. Goodwin (Ed.), *Chemistry and Biochemistry of plant pigments* (pp. 736−778). London: Academic Press.

Hatfield, J. L., Gitelson, A. A., Schepers, J. S., & Walthall, C. L. (2008). Application of spectral remote sensing for agronomic decisions. *Agronomy Journal*, *100*, S-117−S-131.

Jacquemoud, S., Ustin, S. L., Verdebout, J., Schmuck, G., Andreoli, G., & Hosgood, B. (1996). Estimating leaf biochemistry using the PROSPECT leaf optical properties model. *Remote Sensing of Environment*, *56*, 194−202.

Johnson, L. F., Bosch, D. F., Williams, D. C., & Lobitz, B. M. (2001). Remote sensing of vineyard management zones: implication for wine quality. *Applied Engineering in Agriculture*, *17*(4), 557−560.

Johnson, L. F., Roczen, D. E., Youkhana, S. K., Nemani, R. R., & Bosch, D. F. (2003). Mapping vineyard leaf area with multispectral satellite imagery. *Computers and Electronics in Agriculture*, *38*(1), 33−44.

Jolley, V. D., & Brown, J. C. (1994). Genetically controlled uptake and use of iron by plants. In J. A. Manthey, D. E. Crowley, & D. G. Luster (Eds.), *Biochemistry of metal micronutrients in the rhizosphere* (pp. 251−266). : Boca Raton Lewis Publishers.

Kuusk, A. (1995a). A Markov chain model of canopy reflectance. *Agricultural and Forest Meteorology*, *76*, 221−236.

Kuusk, A. (1995b). A fast, invertible canopy reflectance model. *Remote Sensing of Environment*, *51*, 342−350.

Lagacherie, P., Collin-Bellier, C., & Goma-Fortin, N. (2001). Analysing rate and spatial variability of vinestock mortality in a Languedocian vineyard from high resolution aerial photographs. *Journal International des Sciences de la Vigne et du Vin*, *35*(3), 141−148.

Lamb, D. W., Hall, A., & Louis, J. (2001). Airborne remote sensing of vines for canopy variability and productivity. *Australian Grapegrower Winewaker*, *449*, 89−92.

Lamb, D. W., Weedon, M. M., & Bramley, R. G. V. (2004). Using remote sensing to predict grape phenolics and colour at harvest in a Cabernet Sauvignon vineyard: timing observations against vine phenology and optimising image resolution. *Australian Journal of Grape and Wine Research*, *10*, 46−54.

Lanjeri, S., Melia, J., & Segarra, D. (2001). A multi-temporal masking classification method for vineyard monitoring in central Spain. *International Journal of Remote Sensing*, *16*, 3167−3186.

le Maire, G., François, C., & Dufrêne, E. (2004). Towards universal broad leaf chlorophyll indices using PROSPECT simulated database and hyperspectral reflectance measurements. *Remote Sensing of Environment*, *89*, 1−28.

Marschner, H., Romheld, V., & Kissel, M. (1986). Different strategies in higher plants in mobilization and uptake of iron. *Journal of Plant Nutrition*, *9*, 695−713.

Martín, P., Zarco-Tejada, P. J., González, M. R., & Berjón, A. (2007). Using hyperspectral remote sensing to map grape quality in 'Tempranillo' vineyards affected by iron chlorosis. *Vitis*, *46*(1), 7−14.

Martín, P., Zarco-Tejada, P. J., González, R., & González, M. R. (2008). Diagnóstico nutricional y recomendaciones de abonado del viñedo en suelos calizos de la Ribera del Duero. *Vida Rural*, *270*, 26−32.

Meggio, F., Zarco-Tejada, P. J., Miller, J. R., Martín, P., González, M. R., & Berjón, A. (2008). Row orientation and viewing geometry effects on row-structured vine crops for chlorophyll content estimation. *Canadian Journal of Remote Sensing*, *34*(3), 220−234.

Merzlyak, M. N., & Chivkunova, O. B. (2000). Light stress induced pigment changes and evidence for anthocyanin photoprotection in apple fruit. *Journal of Photochemistry and Photobiology B-Biology*, *55*, 154−162.

Merzlyak, M. N., Solovchenko, A. E., & Gitelson, A. A. (2003). Reflectance spectral features and non-destructive estimation of chlorophyll, carotenoid and anthocyanin content in apple fruit. *Postharvest Biological Technology*, *27*, 197−211.

Montero, F. J., Meliá, J., Brasa, A., Segarra, D., Cuesta, A., & Lanjeri, S. (1999). Assessment of vine development according to available water resources by using remote sensing in La Mancha, Spain. *Agricultural Water Management*, *40*, 363−375.

Morales, F., Abadia, A., Belkhodja, R., & Abadiua, I. (1994). Iron deficiency induced changes in the photosynthetic pigment composition of field-grown pear (*Pyrus communis* L.) leaves. *Plant Cell Environment*, *17*, 1159−1160.

OIV. (1996). Résolution VITI 4/95. Diagnostic foliare: une métode harmoniseé. *Bull OIV*, *69*, 779−780.

Peñuelas, J., Baret, F., & Filella, I. (1995). Semi-empirical indices to assess carotenoids/chlorophyll a ratio from leaf spectral reflectance. *Photosynthetica*, *31*, 221−230.

Pérez, M.A. (2002). Tesis Doctoral. Densidad de plantación y riego: aspectos ecofisiológicos, agronómicos y calidad de la uva en c.v. Tempranillo. Instituto Tecnológico Agrario de Castilla y León. 308 pp.

Pirie, A. J. G., & Mullins, M. G. (1980). Concentration of phenolics in the skin of grape berries during fruit ripening and development. *American Journal Enology and Viticulture*, *31*, 34−36.

Ribéreau-Gayon, P., & Glories, Y. (1987). *Phenolics in grapes and wines* (pp. 247−256). Adelaide: Australian Industrial Publishers.Richardson, A. D., Duigan, S. P., & Berlyn, G. P. (1987). An evaluation of noninvasive methods to estimate foliar chlorophyll content. *New Phytologist*, *153*, 185−194.

Richardson, A. D., Duigan, S. P., & Berlyn, G. P. (2002). An evaluation of noninvasive methods to estimate foliar chlorophyll content. *New Phytologist*, *153*, 185−194.

Rock, B. N., Hoshizaki, T., & Miller, J. R. (1988). Comparison of in situ and airborne spectral measurements of the blue shift associated with forest decline. *Remote Sensing of Environment*, *24*(1), 109−127.

Rondeaux, G., Steven, M., & Baret, F. (1996). Optimization of soil-adjusted vegetation indices. *Remote Sensing of Environment*, *55*, 95−107.

Rouse, J.W., Jr., Haas, R.W., Deering, D.W., Schell, J.A., & Harlan J.C. (1974). Monitoring the Vernal Advancement and Retrogradation (Greenwave Effect) of Natural Vegetation. Type III Final Report, NASA Goddard Space Flight Center, Greenbelt, Maryland, 20771, USA, 371 pp.

Suárez, L., Zarco-Tejada, P. J., Sepulcre-Cantó, G., Pérez-Priego, O., Miller, J. R., Jiménez-Muñoz, J. C., & Sobrino, J. (2008). Assessing Canopy PRI For Water Stress Detection With Diurnal Airborne Imagery. *Remote Sensing of Environment*, *112*, 560−575.

Sims, D. A., & Gamon, J. A. (2002). Relationships between leaf pigment content and spectral reflectance across a wide range of species, leaf structures and developmental stages. *Remote Sensing of Environment*, *81*, 337−354.

Singleton, V. L., & Rossi, J. A. (1965). Colorimetry of total phenolics with phosphomolibdic phosphotungstic acid reagents. *American Journal of Enology and Viticulture*, *16*(3), 144−158.

Smart, R. & Robinson, M. (1991). 'Sunlight into wine' Winetitles: Adelaide.

Sobrino, J. A., Jiménez-Munoz, J. C., Zarco-Tejada, P. J., Sepulcre-Cantó, G., & de Miguel, E. (2006). Land surface temperature derived from airborne hyperspectral scanner thermal infrared data. *Remote Sensing of Environment*, *102*, 99−115.

Swain, T., & Hillis, W. E. (1959). The phenolic constituents of Prunus domestica I: the qualitative analysis of phenolic contituents. *Journal of the Science of Food and Agriculture*, *10*, 63−69.

Tagliavini, M., & Rombolà, A. D. (2001). Iron deficiency and chlorosis in orchard and vineyard ecosystems. *European Journal of Agronomy*, *15*, 71−92.

Terry, N., & Abadia, J. (1986). Function of iron in chloroplasts. *Journal of Plant Nutrition*, *9*, 609−616.

Veliksar, S. G., Toma, S. I., & Kreidman, J. (2005). Effect of Fe-containing compounds on the chlorosis manifestation and grape quality. *Proc. International Workshop on Advances in Grapevine and Wine Research, Venosa, Italy*, *vol. 122*,.

Vivas, N., Glories, Y., Lagune, L., Saucier, C., & Augustin, M. (1994). Estimation of the polymerisation level of procyanidins from grapes and wines by use of p-dimethylaminocinnamaldehyde. *Journal International des Sciences de la Vigne et du Vin*, *28*, 319−336.

Vogelmann, J. E., Rock, B. N., & Moss, D. M. (1993). Red edge spectral measurements from sugar maple leaves. *International Journal of Remote Sensing*, *14*, 1563−1575.

Author's personal copy

Wallace, A. (1991). Rational approaches to control of iron deficiency other than plant breeding and choice of resistant cultivars. *Plant Soil*, *130*, 281−288.

Zarco-Tejada, P. J., Miller, J. R., Mohammed, G. H., & Noland, T. L. (2000). Chlorophyll fluorescence effects on vegetation apparent reflectance: I. Leaf-level measurements and simulation of reflectance and transmittance spectra. *Remote Sensing of Environment*, *74*(3), 582−595.

Zarco-Tejada, P. J., Miller, J. R., Mohammed, G. H., Noland, T. L., & Sampson, P. H. (2001). Scaling-up and model inversion methods with narrow-band optical indices for chlorophyll content estimation in closed forest canopies with hyperspectral data. *IEEE Transactions on Geoscience and Remote Sensing*, *39*(7), 1491−1507.

Zarco-Tejada, P. J., Berjón, A., Morales, A., Miller, J. R., Agüera, J., Cachorro, V. (2003). Leaf biochemistry estimation on EU high-value crops with ROSIS and DAIS hyperspectral data and radiative transfer simulation. 3rd EARSeL Workshop on imaging spectroscopy (pp. 597–602). Germany, Munich.

Zarco-Tejada, P. J., Miller, J. R., Morales, A., Berjón, A., & Agüera, J. (2004). Hyperspectral indices and model simulation for chlorophyll estimation in open-canopy tree crops. *Remote Sensing of Environment*, *90*(4), 463−476.

Zarco-Tejada, P. J., Berjón, A., López-Lozano, R., Miller, J. R., Marin, P., Cachorro, V., González, M. R., & de Frutos, A. (2005). Assessing vineyard condition with hyperspectral indices: leaf and canopy reflectance simulation in a row-structured discontinuous canopy. *Remote Sensing of Environment*, *99*, 271−287.